The development of the quaternion wavelet transform

Peter Fletcher, Stephen John Sangwine

www.elsevier.com/locate/sigpro

PII: S0165-1684(16)30378-4
DOI: http://dx.doi.org/10.1016/j.sigpro.2016.12.025
Reference: SIGPRO6353

To appear in: *Signal Processing*

Received date: 22 March 2016
Revised date: 8 December 2016
Accepted date: 26 December 2016

Cite this article as: Peter Fletcher and Stephen John Sangwine, The developmer of the quaternion wavelet transform, *Signal Processing* http://dx.doi.org/10.1016/j.sigpro.2016.12.025

The development of the quaternion wavelet transform

Peter Fletcher*, Stephen John Sangwine

School of Computer Science and Electronic Engineering, University of Essex, Wivenhoe Park, Colchester, CO4 3SQ, United Kingdom.

Abstract

The purpose of this article is to review what has been written on what other authors have called *quaternion wavelet transforms* (QWTs): there is no consensus about what these should look like and what their properties should be. We briefly explain what real continuous and discrete wavelet transforms and multiresolution analysis are and why complex wavelet transforms were introduced; we then go on to detail published approaches to QWTs and to analyse them. We conclude with our own analysis of what it is that should define a QWT as being truly quaternionic and why all but a few of the "QWTs" we have described do not fit our definition.

Keywords: Quaternion wavelet transform, Quaternion STFT.

1. Introduction

In this article we try to show how quaternion wavelet transforms (QWTs) have been developed. Wavelet transforms represent signals using a linear combination of basis functions called *wavelets*, whose principal characteristic is that they are localised in time or space. Unlike a representation using periodic basis

*Corresponding author.
E-mail addresses: pfletc@essex.ac.uk (P. Fletcher), sjs@essex.ac.uk (S. J. Sangwine).

functions such as sines and cosines, wavelet transforms allow localised signal content to be analysed.

As we note at the beginning of section 4, most of the theory about wavelets and wavelet transforms, including that about complex wavelet transforms (ℂWTs) and QWTs, has been developed for real-valued signals and greyscale images.

However, we are concerned with signals and images which require more than one component per sample or pixel, for example quaternion signals and, in particular, colour images represented as arrays of quaternions: QWTs for processing these will have different properties from the majority of the QWTs that have appeared so far. As well as discussing QWTs for quaternion signals and arrays, we also briefly consider ℂWTs for complex signals.

Throughout the paper, when we refer to signals and time, it should also be understood that we may mean images and space (in the sense of position within an image). Most of what we cover generalises to the 2-D case of images.

In section 2 we briefly cover the history of real wavelets and describe their properties. There are three types of wavelet analysis, using continuous wavelets, discrete wavelets and multiresolution analysis, and we discuss each of these in turn. There are some problems with real wavelets and in section 3 we see how complex wavelets were introduced to solve them. In section 4 we survey all articles that have contributed to the development of QWTs and describe what each article's authors have done. There is no single approach to QWTs and in section 5.4 we say what we believe a "true" QWT should and should not look like. In section 6 we present our conclusions.

2. Classical (ℝ-valued) wavelet transforms

We start by reviewing briefly the main ideas of wavelets and wavelet transforms in the real-valued case, in order to provide some context for the rest of the paper. A much fuller treatment is given by, *e.g.*, Kovačević et al. (2014).

2.1. Background

The Fourier transform (FT) gives information about the frequency content of a signal, but nothing about where in time or space its different constituent frequencies occur. In some applications, for example with non-stationary signals where some frequency content is present only for a limited time, it would be desirable to know the distribution of frequencies over time or space, which led to the introduction of the short-time Fourier transform (STFT) by Gabor (1946a). A "sliding window" is introduced into the FT, initially centred at time 0, say; the signal is assumed to be approximately stationary in the window and its FT is found. The window is then shifted by t and the FT of the new section of signal is found, and so on until the whole signal has been covered. In continuous time and frequency the STFT in 1-D, centred on time t, can be expressed as

$$\mathcal{F}_{\text{STFT}} f(\omega, t) = \int_{-\infty}^{\infty} f(s) g(s - t) \mathrm{e}^{-j\omega s} \mathrm{d}s, \tag{1}$$

where $g(\cdot)$ is the window function. In discrete time the STFT becomes

$$F_{\text{STFT}}(\omega, t) = \sum_{m=-\infty}^{\infty} f[m] g[m - t] \mathrm{e}^{-j\omega m}. \tag{2}$$

The function $g(\cdot)$ or $g[\cdot]$ will always be even in practice and some authors would write $g(t - s)$ and $g[t - m]$ above. Gabor experimented with a number of different functions for the window $g(\cdot)$ and found the best he could do was to use a Gaussian; the STFT with this window function is now called the Gabor transform. We cannot know the exact frequency at a given time and Heisenberg's Uncertainty Principle applies per Gabor (1946b):

$$\Delta t \Delta \omega \geqslant \frac{1}{2}, \tag{3}$$

where Δt is the uncertainty in time and $\Delta\omega$ is the uncertainty in angular frequency. The Gabor transform is optimal in the sense that this inequality theo-

retically becomes an equality when $g(\cdot)$ is a Gaussian.

A major drawback of the STFT is that once the window is chosen, its resolution is fixed. There are two extremes to consider: a high frequency signal with a period less than the width of the window and only a few oscillations would have a relatively large uncertainty as to its actual position; and a lower frequency signal with a period longer than the width of the window would not actually be detected at all. Heuristically, the (discrete) wavelet transform is similar to an STFT, but one with a range of different window sizes: a larger number of short windows to capture the detail at higher frequencies and a smaller number of long windows for the lower frequencies.

The term "wavelet" had already been used for many years by geophysicists, *e.g.*, Ricker (1953), to refer to a single component of a seismogram when in the early 1980s, *e.g.*, Grossmann and Morlet (1984), the mathematics of wavelets was developed to allow them to be used as a tool in signal processing. The simplest wavelet is the *Haar wavelet*, which appears to have been so-named in the 1970s or 1980s: Haar (1910) studied systems of orthogonal functions using a set of orthogonal rectangular basis functions, with each basis function consisting of a short positive pulse followed immediately by a short negative pulse:

$$\psi(t) := \begin{cases} 1 & 0 \leqslant t < \frac{1}{2} \\ -1 & \frac{1}{2} \leqslant t < 1 \\ 0 & \text{otherwise.} \end{cases}$$

Later, after the development of wavelets, this Haar wavelet was generalised to $\psi_{\alpha,\beta}(t) := 2^{-\alpha/2}\psi(2^{-\alpha}t - \beta)$, where $\alpha, \beta \in \{0\} \cup \mathbb{Z}^+$.[1] The scale factor $2^{-\alpha/2}$ ensures that $\int_{-\infty}^{\infty} |\psi_{\alpha,\beta}(t)|^2 \, \mathrm{d}t = 1$. $\psi(t)$ is called the *mother wavelet* and the $\psi_{\alpha,\beta}(t)$ functions, *daughter wavelets*; α is a scale parameter and β is a translation

[1] Some authors write $\psi_{\alpha,\beta}(t) = 2^{\alpha/2}\psi(2^{\alpha}t - \beta)$, but the notation we have used is as per Daubechies (1992, p. 10)

parameter.

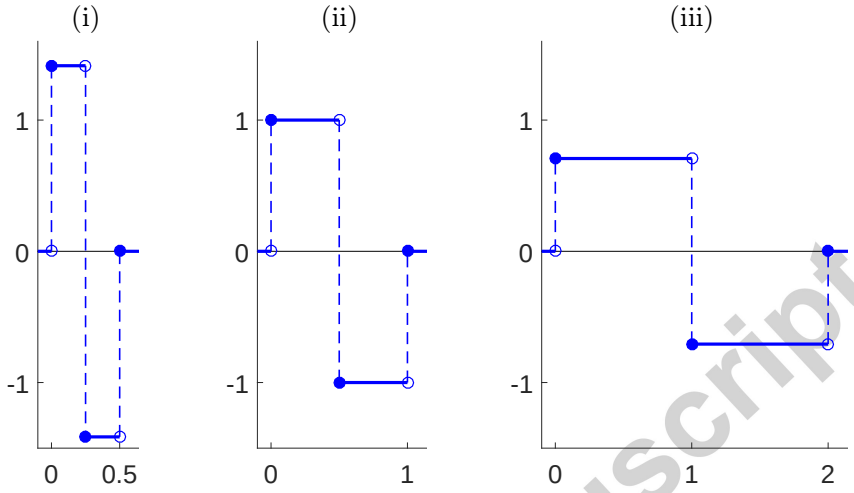

Figure 1: The Haar mother wavelet (ii) and two levels of Haar daughter wavelets: (i) $\psi_{-1,0}(t) = \sqrt{2}\psi(2t)$, (ii), $\psi_{0,0}(t) = \psi(t)$, (iii) $\psi_{1,0}(t) = \frac{1}{\sqrt{2}}\psi\left(\frac{1}{2}t\right)$.

There was little interest in Haar's rectangular pulse until it was picked up by Lévy (1948) as an improvement on the Fourier basis functions for studying the fine detail of Brownian motion: as demonstrated by Pinsky (2001), Brownian motion can be expressed as a sum of Haar wavelets.

A square pulse is not the only wavelet that can be used. Strömberg (2006) started the development of discrete wavelets beyond what Haar had done and Daubechies (1988) introduced families of orthogonal wavelets with compact support. The continuous wavelet transform first appeared in Zweig et al. (1976), although that in Goupillaud et al. (1984) is the oldest which would be recognised today as a wavelet transform.

2.2. Properties of wavelets

Many wavelets have been developed, each with properties suited to particular applications. All have the property of *localisation* in space and time and some have infinite support, but the most popular, as mathematical objects if not for applications according to Blatter (1998, p. 6), have *finite support*. A wavelet

having finite support simply means that there is a finite interval, outside of which its amplitude is zero. A wavelet transform should be able to analyse a signal (or image) at different scales and so the underlying wavelets need to be localised in spatial frequency. It also needs to encode where in time (or space) these frequencies occur and so the wavelets need to be localised in time (or space) as well. A 1-D example of space and time localisation would be a music score, which shows which musical notes and hence sound frequencies need to occur and at what times. Wavelet analysis of the music would theoretically allow the music score to be reconstructed but Fourier analysis of the same music would not, since it would not reveal the locations of different frequency content due to individual notes.

The wavelet functions are chosen from $L^1(\mathbb{R}) \cap L^2(\mathbb{R})$, the space of measurable functions that are absolutely and square integrable:

$$\int_{-\infty}^{\infty} |\psi(t)| \, \mathrm{d}t < \infty, \qquad \text{and} \qquad \int_{-\infty}^{\infty} |\psi(t)|^2 \, \mathrm{d}t < \infty.$$

In addition, a wavelet must have zero mean and a squared norm of unity, so:

$$\int_{-\infty}^{\infty} \psi(t) \mathrm{d}t = 0 \qquad \text{and} \qquad \int_{-\infty}^{\infty} |\psi(t)|^2 \, \mathrm{d}t = 1.$$

We define a wavelet as

$$\psi_{a,b} : \mathbb{R} \to \mathbb{C}, \qquad t \mapsto \frac{1}{\sqrt{a}} \psi \left(\frac{t-b}{a} \right),$$

where $(a, b) \in \mathbb{R}^+ \times \mathbb{R}$ (Blatter, 1998, p. 14). Note that this definition of $\psi_{a,b}$ is slightly different from the one we used for the $\psi_{\alpha,\beta}$ of the Haar wavelet above: if $\psi_{a,b}$ were that Haar wavelet, we would have $a = 2^\alpha$ and $b = 2^\alpha \beta$. Both definitions are in use and we also call a and b the *scale* and *translation* parameters respectively.

2.3. The continuous wavelet transform

The continuous wavelet transform

$$\mathcal{W}_\psi f : \mathbb{R}^+ \times \mathbb{R} \to \mathbb{C}, \qquad (a,b) \mapsto \mathcal{W}_\psi f(a,b)$$

of a signal f is defined as

$$\mathcal{W}_\psi f(a,b) := \langle f, \psi_{a,b} \rangle = \frac{1}{\sqrt{a}} \int_{-\infty}^{\infty} f(t) \overline{\psi\left(\frac{t-b}{a}\right)} \mathrm{d}t, \tag{4}$$

where the variables are as we defined in subsection 2.2. The result is a data array

$$\big(\mathcal{W}_\psi f(a,b) \big| (a,b) \in \mathbb{R}^+ \times \mathbb{R}\big),$$

where, if these data are plotted, a is traditionally taken as the vertical axis and b, the horizontal. Thus, unlike an FT, we transform a 1-D signal into a 2-D result: the inverse transform has to therefore turn the 2-D representation back into 1-D, which requires integration over two variables:

$$f = \frac{1}{C_\psi} \int_{-\infty}^{\infty} \int_{-\infty}^{\infty} \frac{\mathcal{W}_\psi f(a,b) \psi_{a,b}}{a^2} \mathrm{d}a \, \mathrm{d}b,$$

where the scaling factor C_ψ is

$$C_\psi = 2\pi \int_{-\infty}^{\infty} \frac{|\hat{\psi}(\xi)|^2}{|\xi|} \mathrm{d}\xi < \infty$$

and $\hat{\psi}(\cdot)$ denotes the Fourier transform (Blatter, 1998, *pp.* 15/16/61). A derivation of C_ψ can be found in (Daubechies, 1992, *pp.* 24/25).

Incidentally, the Fourier transform itself can be regarded as a particular case of a continuous wavelet transform, with the mother wavelet $\psi(t) = \exp(-2\pi \mathrm{j} t)$.

2.4. The discrete wavelet transform

A discrete wavelet transform (DWT) can be thought of as an all-pass filter, but one made up of separate low-pass and high-pass filters with cut-offs which coincide. One can be implemented, together with its inverse, as a two-channel

filter bank with finite impulse response filters (FIRs), as illustrated in Fig. 2. The processing block in practice might perform *e.g.*, signal compression by suppression of small components, but for the purposes of our discussion here we assume that it has been removed and the outputs of the downsamplers (decimators) go straight into the upsamplers (expanders). The H's are low-pass filters, the G's are high-pass filters and the tildes ($\widetilde{\cdot}$) indicate that the ordering of the filters' coefficients has been reversed. Together the four filters form a quadrature mirror filter (QMF). The passband of a realisable filter can never have a perfect cut-off and where filter responses overlap, aliasing can occur. In a QMF, the aliasing that must occur in the analysis bank is cancelled by the equal and opposite aliasing in the synthesis bank, leading to a perfect reconstruction of the input signal, apart from a delay. The aliasing is actually augmented by the decimators, but this makes it easier to remove.

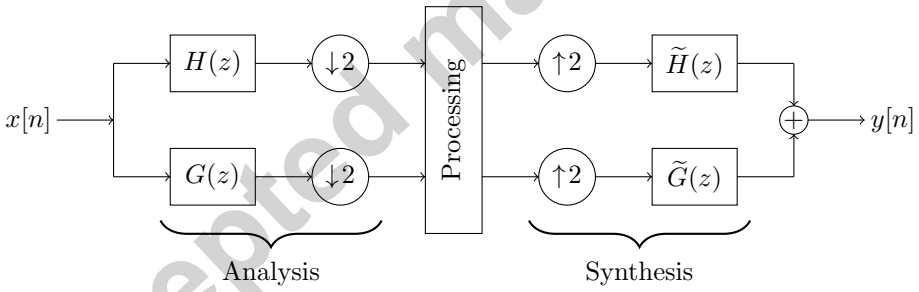

Figure 2: The basic layout of a simple discrete wavelet transform, adapted from (Jaffard et al., 2001, p. 39, Fig. 3.3).

In terms of z-transforms, we find that

$$Y(z) = \frac{1}{2}X(z)[H(z)\widetilde{H}(z) + G(z)\widetilde{G}(z)] + \frac{1}{2}X(-z)[H(-z)\widetilde{H}(z) + G(-z)\widetilde{G}(-z)]$$

The second term is due to the decimation and expansion plus aliasing and we can make it zero by choosing $\widetilde{H}(z) = G(-z)$ and $\widetilde{G}(z) = -H(-z)$.

As an example, let the coefficients of H be $\boldsymbol{h} = (a, b, c, d)$ so that:

$$H(z) = a + bz^{-1} + cz^{-2} + dz^{-3}, \qquad \widetilde{H}(z) = \quad d + cz^{-1} + bz^{-2} + az^{-3},$$
$$G(z) = d - cz^{-1} + bz^{-2} - az^{-3}, \qquad \widetilde{G}(z) = -a + bz^{-1} - cz^{-2} + dz^{-3}.$$

Then after some calculation we find that

$$Y(z) = X(z)[(ac + bd)z^{-1} + (a^2 + b^2 + c^2 + d^2)z^{-3} + (ac + bd)z^{-5}].$$

If $a = -0.1294,\ b = 0.2241,\ c = 0.8365$ and $d = 0.4830$ then $ac + bd = 0$ and $a^2 + b^2 + c^2 + d^2 = 1,$ so that $Y(z) = X(z)z^{-3},$ exactly the same as the input but with a delay. These coefficient values chosen were from the Daubechies db2 wavelet (Weeks, 2011, p. 284), but we could have chosen db3, ..., db45, the Mexican hat wavelet, the Meyer wavelet, *etc.* The coefficient vectors are always even-length and $\boldsymbol{h}$ and $\boldsymbol{g}$ may have different lengths.

For more than one level of decomposition of some input signal, the low-pass output of the first analysis stage would form the input to another analysis stage and the high-pass output would be saved; and so on to whatever level of analysis is desired, as illustrated in Fig. 3 with three levels of analysis: with the input signal $x[n]$, $a[n]$ is the final low frequency approximation and $d[0, n]$, $d[1, n]$ and $d[2, n]$ are the high frequency details extracted at each level. The frequencies in the detail decrease as we go from $d[0, n]$ to $d[1, n]$ to $d[2, n]$.

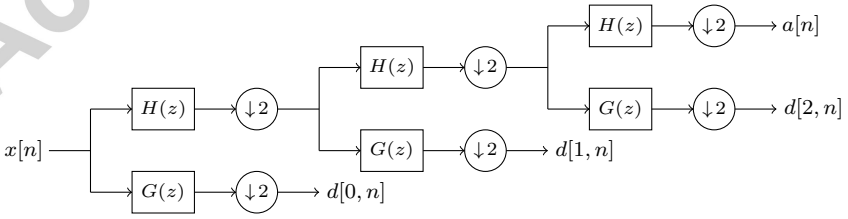

Figure 3: Illustration of multilevel analysis, adapted from Selesnick et al. (2005, Fig. 24(a)).

In Fig. 4 is illustrated the reverse process, with the detail $d'[2, n]$, $d'[1, n]$ and

$d'[0,n]$ added back step-by-step. If no processing has been done between the analysis and synthesis filters so that $d'[2,n] = d[2,n]$, $d'[1,n] = d[1,n]$, $d'[0,n] = d[0,n]$ and $a'[n] = a[n]$, then we would theoretically have $y[n] = x[n]$.

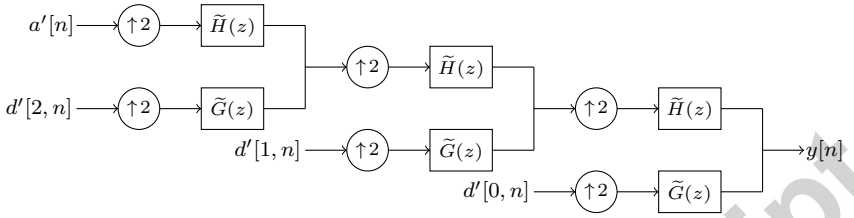

Figure 4: Illustration of multilevel synthesis, adapted from Selesnick et al. (2005, Fig. 24(b)).

Thus, at each stage of analysis, the detail at that scale is stripped off and at each stage of synthesis, the detail at that scale is added back in.

In recent years, wavelet transforms have found applications in video and internet communications compression, object recognition and numerical analysis. As an example of image compression, the JPEG2000 image compression standard, described by Taubman and Marcellin (2002), uses CDF 5/7 and CDF 9/7 wavelets, which are two versions of the Cohen-Daubechies-Feauveau wavelet.

2.5. Multiresolution analysis

Multiresolution analysis (MRA) was developed by Mallat (1989a,b) and Meyer (1992 English edition) as a design method for scaling functions and wavelets. The idea is that a function is viewed at the finest resolution and decomposed into the detail at that resolution plus a complementary approximation; this approximation is then viewed at a lower resolution and decomposed into the detail at the new resolution plus a new approximation; and so on. This is a similar idea to the multilevel analysis described in the previous subsection. Much of this subsection is adapted from Goswami and Chan (2011, *pp.* 89-94).

2.5.1. Multiresolution spaces

With MRA, we consider the spaces, to which the detail and approximation functions resulting from a multilevel analysis, have to belong. We can then develop conditions that these functions must obey. Let the subspace $\boldsymbol{V}_s$ be generated by the bases $\{\phi_{k,s}\colon 2^{-s/2}\phi(2^{-s}t-k); k\in\mathbb{Z}\}$ and the subspace $\boldsymbol{W}_s$ by $\{\psi_{k,s}\colon 2^{-s/2}\psi(2^{-s}t-k); k\in\mathbb{Z}\}$, so that any function $x_s(t)\in\boldsymbol{V}_s$, say, can be approximated (in an L^2 sense) by a linear combination of $\phi_{k,s}$ for a finite set of different k's; and similarly for any function $y_s(t)\in\boldsymbol{W}_s$, say, and $\psi_{k,s}$. As with the multilevel analysis, both $x_{s+1}(t)\in\boldsymbol{V}_{s+1}$ and $y_{s+1}(t)\in\boldsymbol{W}_{s+1}$ can be obtained from $x_s(t)$.

In the following, we define for $a\in\mathbb{R}^+$,

$$D_a:\quad \psi\mapsto D_a\psi,\qquad D_a\psi(t):=\psi\left(\frac{t}{a}\right).$$

From Blatter (1998, *pp.* 121/2), a multiresolution analysis has the following ingredients.

1. A bilateral sequence $(\boldsymbol{V}_j, j\in\mathbb{Z})$ of closed subspaces of $L^2(\mathbb{R})$. These $\boldsymbol{V}_j$ are ordered by inclusion,

$$\{0\}\ldots\subset\boldsymbol{V}_2\subset\boldsymbol{V}_1\subset\boldsymbol{V}_0\subset\boldsymbol{V}_{-1}\subset\ldots\boldsymbol{V}_j\subset\boldsymbol{V}_{j-1}\subset\ldots\subset L^2(\mathbb{R}) \qquad (5)$$

(smaller values of j correspond to larger spaces $\boldsymbol{V}_j$), and one has

$$\bigcap_j \boldsymbol{V}_j=\{0\}\qquad\text{(separation axiom)}$$

$$\overline{\bigcup_j \boldsymbol{V}_j}=L^2(\mathbb{R})\quad\text{(completeness axiom)}$$

The time signals $x\in\boldsymbol{V}_j$ only comprise features (details) exhibiting a spread of size $\geqslant 2^j$ on the time axis. The more negative j is, the finer are the details that may occur in an $x\in\boldsymbol{V}_j$, and "in the limit" every single $x\in L^2(\mathbb{R})$ can be attained by functions $x_j\in\boldsymbol{V}_j$.

2. The $\boldsymbol{V}_j$ are connected to each other by a rigid scaling property:

$$\boldsymbol{V}_{j+1} = D_2(\boldsymbol{V}_j) \qquad \forall j \in \mathbb{Z}.$$

Referring to time signals x, this can be expressed as follows:

$$x \in \boldsymbol{V}_j \Leftrightarrow x(2^j \cdot) \in \boldsymbol{V}_0.$$

3. $\boldsymbol{V}_0$ contains one basis vector per base step 1. To be precise, there is a function $\phi \in L^2 \cap L^1$ such that its translates $(\phi(\cdot - k), k \in \mathbb{Z})$ form an orthonormal basis of $\boldsymbol{V}_0$. This function ϕ is commonly called the *scaling function* of the MRA under consideration; it is the determining element of the whole set-up.

Some authors reverse the ordering of the $\boldsymbol{V}_j$ in equation (5).

Each $\boldsymbol{V}_s$ is a proper subspace of $\boldsymbol{V}_{s-1}$ and the orthogonal complement of $\boldsymbol{V}_s$ in $\boldsymbol{V}_{s-1}$ is called $\boldsymbol{W}_s$, the wavelet subspace, satisfying

$$\boldsymbol{V}_s \cap \boldsymbol{W}_s = \{0\} \quad s \in \mathbb{Z}$$
$$\boldsymbol{V}_s \oplus \boldsymbol{W}_s = \boldsymbol{V}_{s-1},$$

where the symbol $\oplus$ means the direct sum. This leads to

$$V_s = \bigoplus_{\ell=s+1}^{\infty} \boldsymbol{W}_\ell.$$

The $\{\boldsymbol{V}_s\}$ are nested and the $\{\boldsymbol{W}_s\}$ are (according to Goswami and Chan)

"mutually orthogonal"[2] and together satisfy

$$\begin{aligned} \boldsymbol{V}_\ell \cap \boldsymbol{V}_m &= \boldsymbol{V}_\ell, \quad && \ell > m \\ \boldsymbol{W}_\ell \cap \boldsymbol{W}_m &= \{0\}, && \ell \neq m \\ \boldsymbol{V}_\ell \cap \boldsymbol{W}_m &= \{0\}, && \ell \geqslant m. \end{aligned}$$

The way $\boldsymbol{V}_s$ and $\boldsymbol{W}_s$ are related as s changes is illustrated in Fig. 5.

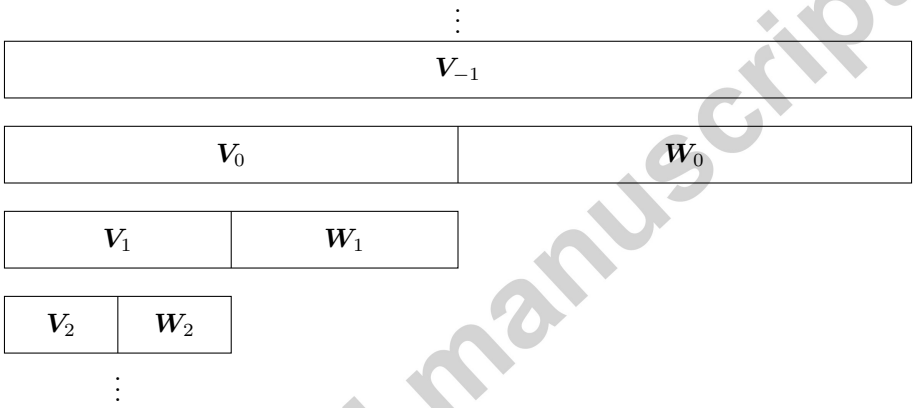

Figure 5: Illustration of splitting of MRA subspaces, adapted from Goswami and Chan (2011, p. 97 Fig. 5.2).

2.5.2. Orthogonal decomposition

If we insist that $\boldsymbol{W}_s \perp \boldsymbol{V}_s$, we then have an *orthogonal decomposition*. This implies that, *e.g.*, for $s = 0$,

$$\int_{-\infty}^{\infty} \phi(t)\psi(t-\ell)\mathrm{d}t = 0, \quad \forall \ell \in \mathbb{Z}.$$

A *Riesz basis* of a space is one where the basis vectors are normalised and linearly independent per Mallat (2009, p. 22). The sets $\{\phi(t-k) : k \in \mathbb{Z}\}$ and $\{\psi(t-k) : k \in \mathbb{Z}\}$ need not be orthogonal in themselves, but we still need the integer translates of ϕ to form a Riesz basis for $\boldsymbol{V}_0$.

[2]We discuss the assumption of orthogonality in section 2.5.2.

2.5.3. Biorthogonal decomposition

Biorthogonal wavelets are a generalisation of orthogonal wavelets. They were introduced by Cohen et al. (1992) and increase the number of degrees of freedom available for filter design; they make perfect reconstruction and linear phase possible simultaneously, while also allowing filter lengths to differ.

If we do not insist that $\boldsymbol{W}_s \perp \boldsymbol{V}_s$ but assume that $\psi_{k,s} \in \boldsymbol{W}_s$ has a dual $\widetilde{\psi}_{k,s} \in \widetilde{\boldsymbol{W}}_s$, this leads to Cohen *et al.*'s biorthogonality condition,

$$\left\langle \psi_{j,k}, \widetilde{\psi}_{\ell,m} \right\rangle = \delta_{j,\ell} \cdot \delta_{k,m}, \qquad j,k,\ell,m \in \mathbb{Z}. \tag{6}$$

We do now need $\widetilde{\boldsymbol{W}}_s \perp \boldsymbol{V}_s$.

The scaling function also has a dual, $\widetilde{\phi}_{k,s} \in \widetilde{\boldsymbol{V}}_s$ and there is another MRA

$$\{0\} \ldots \subset \widetilde{\boldsymbol{V}}_2 \subset \widetilde{\boldsymbol{V}}_1 \subset \widetilde{\boldsymbol{V}}_0 \subset \widetilde{\boldsymbol{V}}_{-1} \subset \ldots \widetilde{\boldsymbol{V}}_j \subset \widetilde{\boldsymbol{V}}_{j-1} \subset \ldots \subset L^2(\mathbb{R})$$

such that $\boldsymbol{W}_s \perp \widetilde{\boldsymbol{V}}_s$.

In the same way that $\boldsymbol{V}_s$ and $\boldsymbol{W}_s$ are related, $\widetilde{\boldsymbol{V}}_s$ and $\widetilde{\boldsymbol{W}}_s$ satisfy

$$\left.\begin{aligned} \widetilde{\boldsymbol{V}}_\ell &= \widetilde{\boldsymbol{V}}_m + \widetilde{\boldsymbol{W}}_m, \\ \widetilde{\boldsymbol{V}}_m \cap \widetilde{\boldsymbol{V}}_\ell &= \widetilde{\boldsymbol{V}}_m, \end{aligned}\right\} \quad m > \ell$$

$$\widetilde{\boldsymbol{W}}_m \cap \widetilde{\boldsymbol{W}}_\ell = \{0\}, \qquad m \neq \ell$$

$$\widetilde{\boldsymbol{V}}_m \cap \widetilde{\boldsymbol{W}}_\ell = \{0\}, \qquad m \geqslant \ell.$$

$$\left.\begin{aligned} \boldsymbol{W}_\ell \perp \widetilde{\boldsymbol{V}}_\ell &\Rightarrow \widetilde{\boldsymbol{V}}_\ell \cap \boldsymbol{W}_m = \{0\}, \\ \widetilde{\boldsymbol{W}}_\ell \perp \boldsymbol{V}_\ell &\Rightarrow \boldsymbol{V}_\ell \cap \widetilde{\boldsymbol{W}}_m = \{0\}, \end{aligned}\right\} \quad m \leqslant \ell.$$

We can now show how dual wavelets, which are sometimes called analysing wavelets, are used to find the coefficients of the original wavelets, which are sometimes called synthesis wavelets. Since

$$\boldsymbol{V}_s = \sum_{n=1}^{N} \boldsymbol{W}_{s+n} + \boldsymbol{V}_{s+N},$$

if $x_M(t) \in \boldsymbol{V}_s$, we have

$$x_M(t) = \sum_{n=1}^{N} y_{M+n}(t) + x_{M+N}(t), \tag{7}$$

where $x_{M+N}(t)$ is the coarsest approximation of $x_M(t)$, and

$$\begin{aligned} x_s(t) &= 2^{-s/2} \sum_{\ell} a_{\ell,s} \phi(2^{-s}t - \ell) \in \boldsymbol{V}_s \\ y_s(t) &= 2^{-s/2} \sum_{\ell} w_{\ell,s} \psi(2^{-s}t - \ell) \in \boldsymbol{W}_s. \end{aligned} \tag{8}$$

Taking the inner product of equation (7) with $\widetilde{\psi}_{k,s}(t)$ gives

$$\left\langle x_M(t), \widetilde{\psi}_{k,s}(t) \right\rangle = \sum_{n=1}^{N} \left\langle y_{M+n}(t), \widetilde{\psi}_{k,s}(t) \right\rangle + \left\langle x_{M+N}(t), \widetilde{\psi}_{k,s}(t) \right\rangle.$$

Since $x_{M+N}(t) \in \boldsymbol{V}_{s+N}$, $\widetilde{\psi}_{k,s}(t) \in \widetilde{\boldsymbol{W}}_s$ and $\boldsymbol{V}_{s+N}$ is orthogonal to $\widetilde{\boldsymbol{W}}_s$, the second inner product on the RHS of this equation is 0. Using Equation (8) to replace $y_{M+n}(t)$ then gives

$$\left\langle x_M(t), \widetilde{\psi}_{k,s}(t) \right\rangle = \sum_{n=1}^{N} \left(\sum_{\ell} w_{\ell,M+n} \left\langle 2^{-(M+n)/2} \psi\left(2^{-(M+n)}t - \ell\right), \widetilde{\psi}_{k,s}(t) \right\rangle \right).$$

Using Equation (6), most of the terms in the expansion of the sum on the RHS of this equation are zero, except the term where $M + n = s$ and $\ell = k$, so that

$$\begin{aligned} \left\langle x_M(t), \widetilde{\psi}_{k,s}(t) \right\rangle &= w_{k,s} \left\langle \psi_{k,s}(t), \widetilde{\psi}_{k,s}(t) \right\rangle \\ &= w_{k,s} \left(\delta_{k,k} \cdot \delta_{s,s}\right) = w_{k,s}. \end{aligned}$$

Therefore we can analyse a function x_M and find its wavelet coefficients by finding its inner product with the dual wavelet $\widetilde{\psi}$.

One advantage of biorthogonal wavelets is that we can have compactly supported symmetric analysis and synthesis wavelets and scaling functions. A continuous orthonormal basis cannot satisfy all of these conditions at the same time. Also, according to Chui and Wang (1995), higher order orthonormal scal-

ing functions and wavelets have poor time-scale localisation.

3. The Dual-Tree Complex wavelet transform

It is natural to ask whether the concepts of wavelets (localisation in time) and wavelet transforms (MRA) can be extended to complex signals, *i.e.*, signals where each sample is a complex value rather than a real one. Such signals provide an intermediate between real and quaternion and other hypercomplex signals: they are therefore worthy of study, in order to suggest generalisations from the real case which may be of significant practical use. In fact, there appears not to have been any recent work done on generalising either wavelets or wavelet transforms to the complex case. Some work has been done using wavelets with complex coefficients to analyse real signals, but we do not look at this. However, there has been some significant work done with complex wavelets in a different sense: as we show in this section, the dual-tree complex wavelet transform exists to overcome serious problems with the real-valued wavelet transform, namely the sensitivity of its coefficients to small time shifts.

The complex wavelet transform (ℂWT) first appeared in published form in Kingsbury and Magarey (1998). The authors discuss the major drawback of the DWT that the ℂWT was introduced to overcome, namely the DWT's sensitivity to small shifts in the input signal: *e.g.*, if an impulse is the input to the filter bank in Fig. 2 and it is shifted by a small amount, then the wavelet coefficients at the outputs of the analysis stage change dramatically, as illustrated in Fig. 6. The inputs here were vectors of 128 zeros with unit impulses at positions 60 and 64 respectively; they are labelled by their squared norms, which give measures of their energies: the second output has roughly twice the energy of the first. The non-translation invariance of wavelets subspaces has been studied by a number of authors, *e.g.*, Hogan and Lakey (2009).

Selesnick et al. (2005) add three more problems with real wavelets:

- oscillations around singularities result in large and small wavelet coefficients that may be positive, negative or close to zero;
- aliasing might occur in the set-up in Fig. 2, even if the filter coefficients are chosen such that aliasing should not occur if thresholding, filtering or quantisation in the processing step upsets the balance between the forward and inverse transforms;
- and Fourier sinusoids in higher dimensions are directional plane waves, but multidimensional real wavelets do not have this property, complicating the processing of geometric image features such as edges.

Selesnick *et al.* noted that the Fourier transform does not suffer from these problems and asked why this was. The answer was that the DWT is based on real oscillating wavelets, whereas the Fourier transform is based on the complex exponential (oscillating sinusoids),

$$\exp(\mathbf{j}\Omega t) = \cos(\Omega t) + \mathbf{j}\sin(\Omega t),$$

where the real cosine and imaginary sine together form a Hilbert transform pair, the imaginary part being the Hilbert transform of the real part.

The Hilbert transform $\mathcal{H}x(t)$ of a signal $x(t)$ is defined as

$$\mathcal{H}x(t) = \frac{1}{\pi}\int_{-\infty}^{\infty}\frac{x(s)}{t-s}\mathrm{d}s.$$

This equation is not very illuminating, but its effect is to introduce a $-\pi/2$ phase shift for the positive frequency components of the input signal: *e.g.*, $\cos(\Omega t - \pi/2) = \sin(\Omega t)$ as above.

As with the Euler expansion, a complex wavelet has a complex-valued scaling function and a complex-valued wavelet of the forms

[3] Adapted from the top pair of plots on `uk.mathworks.com/help/wavelet/examples/dual-tree-wavelet-transforms.html`.

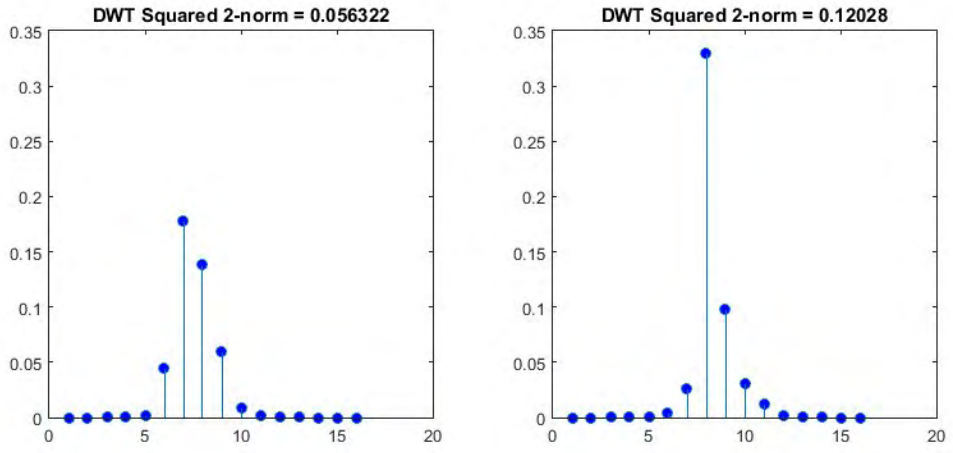

Figure 6: Absolute values of the detail outputs from a level 3 DWT with symlet 7 coefficients; inputs were unit impulses in both cases, but one input had its impulse offset by four sample periods relative to the other.[3]

$$\phi_c(t) = \phi_r(t) + \mathbf{j}\phi_i(t)$$

$$\psi_c(t) = \psi_r(t) + \mathbf{j}\psi_i(t).$$

The real functions $\phi_r(t)$ and $\psi_r(t)$ are even and the imaginary ones $\phi_i(t)$ and $\psi_i(t)$ are odd and, as long as the latter two functions are the respective Hilbert transforms of the former, these form two Hilbert transform pairs and $\phi_c(t)$ and $\psi_c(t)$ are analytic signals as per Ville (1948), which are supported on only one half of the frequency axis.

However, perfectly analytic wavelets and perfect reconstruction are mutually exclusive. The reason why is explained by Selesnick et al. (2005, p. 127). The way found by Kingsbury (1998) to implement the ℂWT was to construct two separate trees of filter banks, each satisfying the perfect reconstruction condition in themselves, but which jointly produce a complex wavelet and scaling function that are as close as possible to being analytic while not being exactly analytic.

Fig. 7 illustrates the set-up for the analysis side of this dual-tree ℂWT. One tree gives the real part of the transform and the other, the imaginary part with

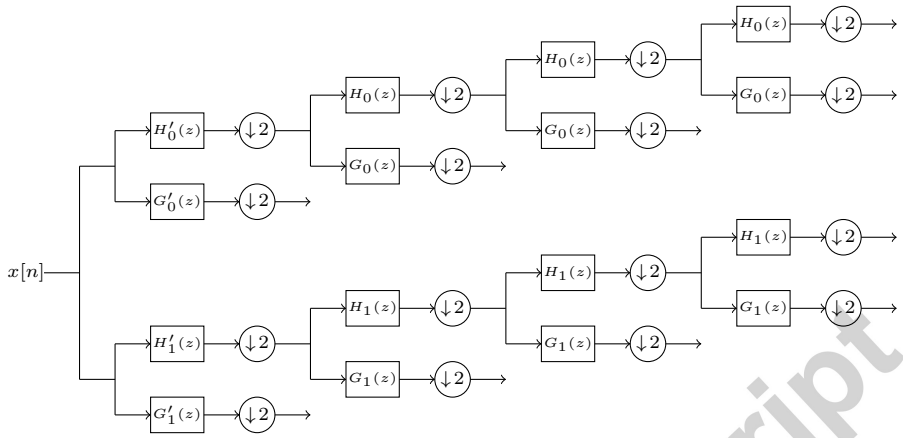

Figure 7: Analysis filter bank for the dual-tree ℂWT, adapted from Selesnick et al. (2005, Fig. 13).

a $-\pi/2$ phase shift relative to the real part. As described with the real DWT, the high-frequency outputs from the G filters are saved, to be added back in on the synthesis side, which is basically the mirror image of the analysis side but with $\widetilde{H}$ and $\widetilde{G}$ filters designed for perfect reconstruction. The first two pairs of filters (marked H' and G') differ from the rest due to their having to cope with the same real input and to introduce the phase difference.

This dual-tree ℂWT was built from two real wavelet transforms, meaning that all the pre-existing theory and practice of designing real wavelet transforms could be used for these new filters.

Fig. 8 shows the result of processing the same impulses as were used to produce Fig. 6, but with a dual-tree ℂWT instead of a DWT: the energies now differ by roughly 2.5%, showing the reduction in shift variance. If the outputs were perfectly analytic there would be no difference at all in the energies.

This ℂWT was an improvement on the DWT, but as we have suggested, was still not perfect for all potential applications.

[4] Adapted from the bottom pair of plots on `uk.mathworks.com/help/wavelet/examples/dual-tree-wavelet-transforms.html`.

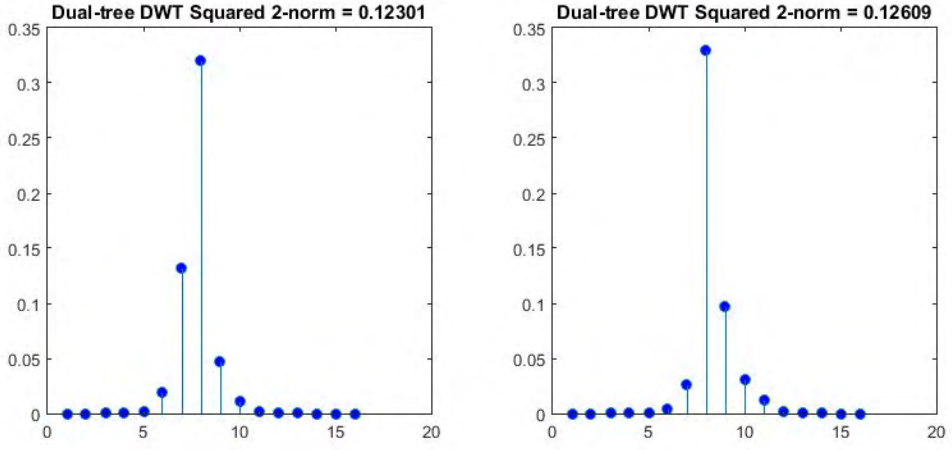

Figure 8: Absolute values of the complex detail outputs from a level 3 dual tree ℂWT with Kingsbury Q-shift coefficients ($\mathrm{Q} = \frac{1}{4}$ or $\frac{3}{4}$ of a sample period); inputs were unit impulses in both cases, but one input had its impulse offset by four sample periods relative to the other.[4]

As noted by Bülow (1999, p. 2), there is a close correspondence between the local structure of a signal and its local phase, and this correspondence had been used in the past in texture analysis and disparity estimation. A ℂWT cannot be used for these types of analysis because being complex, it automatically has one phase, which is useful for analysis in one direction only. As noted by Soulard and Carré (2011), phase with the 2-D version of the ℂWT is ambiguous. This is where Bülow's work comes in: his quaternionic Gabor filter is equivalent to two complex Gabor filters, from which any ambiguity is removed by their having different $\sqrt{-1}$'s in their imaginary parts; recall from subsection 2.1 that a Gabor transform is basically an STFT with a Gaussian window. He studied the phase concept in Chapter 3 of his thesis, Bülow (1999, *pp.* 59-109), and his filter initiated a large body of work on quaternion wavelet transforms (QWTs). We look at these in the next section, after mentioning the few earlier attempts at a QWT.

4. Quaternion wavelet transforms

In this section we review the literature on QWTs. There are a number of different definitions and we shall look in detail particularly at those from the most-cited papers as per the Web of Science: Bayro-Corrochano (2006) with over 30 citations, Zhou et al. (2007) with over 25 and Chan et al. (2008) with over 50. These totals actually include citing articles where the three papers are mentioned only in passing and we omit discussion of them in what follows.

We have not split up this section into separate subsections for continuous and discrete QWTs and quaternion MRAs, but we have attempted to group papers together in a logical fashion, roughly chronologically. The vast majority of QWTs we describe are suitable only for real-valued signals and greyscale images, but we mention colour in relation to a few QWTs in subsection 4.5.

4.1. Early papers

Mitrea (1994, ch. 2) introduced Clifford wavelets and a Clifford multiresolution analysis: the Clifford Algebra $C\ell(0,2)$ is isomorphic to the quaternions. As a specific example, he constructed theoretical Haar Clifford wavelets. He applied the Haar wavelet construction to prove the boundedness of the Cauchy integral operator for Clifford-valued functions on a Lipshcitz surface and noted applications to classical boundary-value problems for the Laplacian on Lipschitz domains.

Traversoni (1995) represented the four components of a quaternion as real wavelets and proposed using this formulation in Navier Stokes problems to express vorticity using all four dimensions. The energy would then be expressed as wavelets and low energy turbulence could be filtered out by suppressing the corresponding wavelets. This idea was not developed further and in Traversoni (2001a) the author used the ideas of Mitrea to obtain a quaternion multiresolution analysis and Haar quaternion wavelet, the latter based on a cubic repre-

sentation of the Haar square pulse in 3-D. In Traversoni (2001b), he applied his Haar quaternion wavelets to image analysis, creating a 3-D representation of a collection of 2-D tomography data.

Bülow (1999) developed a quaternion Hilbert transform and used the polar representation of a quaternion in a quaternionic Gabor filter, on which a large body of research has been based. We review this research in subsections 4.2, 4.3 and 4.4.

4.2. QWTs based on a quaternion Gabor transform

Bayro-Corrochano (2006) introduced a 2-D quaternion MRA, a "wavelet pyramid", which is also covered in Moya-Sánchez and Bayro-Corrochano (2010):

$$f(x,y) = \boldsymbol{A}_n f(x,y) + \sum_{j=1}^{n} [\boldsymbol{D}_{j,H} f(x,y) + \boldsymbol{D}_{j,V} f(x,y) + \boldsymbol{D}_{j,D} f(x,y)],$$

where the approximations $\boldsymbol{A}$ and detail $\boldsymbol{D}$ are defined as

$$\boldsymbol{A}_j f(x,y) = \sum_{k=-\infty}^{\infty} \sum_{\ell=-\infty}^{\infty} a_{j,k,\ell} \boldsymbol{\Phi}_{j,k,\ell}(x,y),$$

$$\boldsymbol{D}_{j,p} f(x,y) = \sum_{k=-\infty}^{\infty} \sum_{\ell=-\infty}^{\infty} d_{j,p,k,\ell} \boldsymbol{\Psi}_{j,p,k,\ell}(x,y)$$

with

$$\boldsymbol{\Phi}_{j,k,\ell}(x,y) = \frac{1}{2^j} \boldsymbol{\Phi}\left(\frac{x-k}{2^j}, \frac{y-\ell}{2^j}\right), \qquad (j,k,\ell) \in \mathbb{Z}^3,$$

$$\boldsymbol{\Psi}_{j,p,k,\ell}(x,y) = \frac{1}{2^j} \boldsymbol{\Psi}_p\left(\frac{x-k}{2^j}, \frac{y-\ell}{2^j}\right)$$

and

$$a_{j,k,\ell}(x,y) = \langle f(x,y), \boldsymbol{\Phi}_{j,k,\ell}(x,y) \rangle,$$

$$d_{j,p,k,\ell} = \langle f(x,y), \boldsymbol{\Psi}_{j,p,k,\ell}(x,y) \rangle.$$

He also decomposed the scaling and wavelet functions into 1-D functions:

$$\begin{aligned}\boldsymbol{\Phi}(x,y) &= \phi(x)\phi(y),\\ \boldsymbol{\Psi}_H(x,y) &= \phi(x)\psi(y),\\ \boldsymbol{\Psi}_V(x,y) &= \psi(x)\phi(y),\\ \boldsymbol{\Psi}_D(x,y) &= \psi(y)\psi(x).\end{aligned}$$

The way this "wavelet pyramid" works is that given a 2-D image $f(x,y)$, for each level j we have four matrices $\boldsymbol{A}_j$, $\boldsymbol{D}_p$, $p = H, V, D$ with elements $\boldsymbol{A}_j(k,\ell) = a_{j,k,\ell}$ and $\boldsymbol{D}_{j,p}(k,\ell) = d_{j,p,k,\ell}$.

For his QWT, Bayro-Corrochano (2006) used two quaternionic modulated Gabor filters in quadrature:

$$\begin{aligned}h^q &= \frac{1}{\sigma_h\sqrt{2\pi}}\exp\left(-\frac{x^2+(\varepsilon y)^2}{\sigma_h^2}\right)\exp\left(\mathbf{i}\frac{C_{hH}\,\omega_{hH}\,x}{\sigma_h}\right)\exp\left(\mathbf{j}\frac{C_{hV}\,\omega_{hV}\,\varepsilon y}{\sigma_h}\right)\\ &= h^q_{ee} + h^q_{oe}\mathbf{i} + h^q_{eo}\mathbf{j} + h^q_{oo}\mathbf{k} \qquad (9)\end{aligned}$$

and

$$\begin{aligned}g^q &= \frac{1}{\sigma_g\sqrt{2\pi}}\exp\left(-\frac{x^2+(\varepsilon y)^2}{\sigma_g^2}\right)\exp\left(\mathbf{i}\frac{C_{gH}\,\omega_{gH}\,x}{\sigma_g}\right)\exp\left(\mathbf{j}\frac{C_{gV}\,\omega_{gV}\,\varepsilon y}{\sigma_g}\right)\\ &= g^q_{ee} + g^q_{oe}\mathbf{i} + g^q_{eo}\mathbf{j} + g^q_{oo}\mathbf{k}, \qquad (10)\end{aligned}$$

where ε is the aspect ratio, the σ's are standard deviations, the ω's are modulation frequencies, $C_{aB} = \omega_{aB}\,\sigma_a$ with $a = h$ or g for low- or high-pass and $B = H$ or V for horizontal or vertical, *ee* means even-even, *eo* means even-odd, *oe* means odd-even and *oo* means odd-odd. These last four come from the cosine and sine products of the equations' expanded exponentials. These filters are quaternionic versions of the low-pass filter H and high-pass filter G of Fig. 2.

Bayro-Corrochano gives conditions on the frequencies as follows:

$$\omega_{hH} + \omega_{hV} = \pi, \quad \omega_{hH} > \omega_{hV}, \quad \omega_{hH} = 3\,\omega_{gH}, \quad \omega_{hH} = \frac{5\pi}{6} \quad \text{and} \quad \omega_{gH} = \frac{\pi}{6}$$

(we have changed some of the notation to avoid using tildes to indicate different constants and to give more meaning to the subscripts).

This quaternion wavelet also appeared in Bayro-Corrochano (2005) and joint conference paper Bayro-Corrochano and de La Torre Gomora (2004) and while he did include Bülow (1999) in these two papers' and his 2006 paper's references, he did not explicitly state that equations (9) and (10) come directly from Bülow's equation (3.40) for a quaternionic Gabor filter.

Despite all the citations, only a few researchers have actually done anything with this QWT. Naouai et al. (2011) used it in the extraction of road map information from high resolution remotely sensed images: conventional methods for updating road maps rely on human intervention and are expensive and time consuming. Ding et al. (2012) analysed black and white images in preparation for colourisation. Chen et al. (2013) developed a new image quality assessment metric for colour images based on phase congruency. Feng et al. (2014) used phase congruency for edge saliency map extraction and image blur measurement.

4.3. QWTs for phase-based stereo matching

Xu et al. (2005) worked on phase-based stereo matching for uncalibrated images. They revised and expanded their work in Xu et al. (2007), Traversoni and Xu (2007) and Zhou et al. (2007), extending the work of Bayro-Corrochano to symmetric/asymmetric biorthogonal wavelet bases in order to build linear-phase quaternion wavelet filters (LPQWFs). Given the scaling function $\phi_{\ell,m}(x)$ and the wavelet base $\psi_{\ell,m}(x)$ of a biorthogonal wavelet, where ℓ denotes the scale factors 2^ℓ, $\ell = 0, 1, \ldots, K$ and $m \in \mathbb{Z}$, the offsets from the origin, four corresponding 1-D analytic wavelets $\psi^H_{\ell,m}(x)$, $\psi^V_{\ell,m}(y)$, $\phi^H_{\ell,m}(x)$ and $\phi^V_{\ell,m}(y)$ can

be built as:

$$\psi^H_{\ell,m}(x) = \psi_{\ell,m}(x) + \mathbf{i}\mathcal{H}_x(\psi_{\ell,m}(x))$$
$$\psi^V_{\ell,m}(y) = \psi_{\ell,m}(y) + \mathbf{j}\mathcal{H}_y(\psi_{\ell,m}(y))$$
$$\phi^H_{\ell,m}(x) = \phi_{\ell,m}(x) + \mathbf{i}\mathcal{H}_x(\phi_{\ell,m}(x))$$
$$\phi^V_{\ell,m}(y) = \phi_{\ell,m}(y) + \mathbf{j}\mathcal{H}_y(\phi_{\ell,m}(y)),$$

where $\mathcal{H}_x(\cdot)$ and $\mathcal{H}_y(\cdot)$ denote the partial Hilbert transforms along the x-axis and y-axis and H and V refer to horizontal and vertical respectively.

The 2-D scale function $\Phi^q(x,y)$ and its three associated quaternion wavelet functions $\Psi^q_H(x,y)$, $\Psi^q_V(x,y)$ and $\Psi^q_D(x,y)$ can then be built as:

$$\Phi^q(x,y) = \phi_{\ell,m}(x)\phi_{\ell,m}(y)$$
$$\Psi^q_H(x,y) = \phi^H_{\ell,m}(x)\psi^V_{\ell,m}(y)$$
$$\Psi^q_V(x,y) = \psi^H_{\ell,m}(x)\phi^V_{\ell,m}(y)$$
$$\Psi^q_D(x,y) = \psi^H_{\ell,m}(x)\psi^V_{\ell,m}(y),$$

where D refers to diagonal. $\Phi^q(x,y)$ is a real 2-D scale function and expanding the three wavelet equations leads to 12 products that can be written succinctly as:

$$\begin{aligned}\Psi^q_P(x,y) = {} & \psi^P(x,y) \\ & + \mathbf{i}\mathcal{H}_x\left(\psi^P(x,y)\right) \\ & + \mathbf{j}\mathcal{H}_y\left(\psi^P(x,y)\right) \\ & + \mathbf{k}\mathcal{H}_{xy}\left(\psi^P(x,y)\right),\end{aligned}$$

where $\mathcal{H}_{xy}(\cdot)$ denotes the total Hilbert transform and $\psi^P(x,y)$, $P \in \{H,V,D\}$ is a general 2-D real wavelet with different orientations. Thus each quaternion wavelet consists of a Hilbert quadruple and is suited to the construction of 2-D

analytic signals.

Zhou *et al.* developed a practical technique for constructing their LPQWFs using real biorthogonal bases. They used a cost function approach, minimisation of which avoided false matches in their stereo matching algorithm.

Despite the relatively high number of citations mentioned in the introduction, all the papers citing Zhou et al. (2007) appear to report something other than any extension to or application of their QWT.

4.4. The dual tree quaternion wavelet transform

The dual tree QWT was introduced in Chan et al. (2004b). It went through several refinements in Chan et al. (2004a), Chan et al. (2005) and Chan et al. (2006), culminating in Chan et al. (2008). In table 1, we analyse by application all the articles up to 2015 that make use of this version of the QWT. Chan *et al.* themselves used it for edge geometry estimation and image disparity estimation and have made their MATLAB® code for the latter, including that for their QWT, available on the website of the Digital Signal Processing Group at Rice University.[5] This QWT is based on the 2-D analytic signal of Bülow (1999):

Definition 4.1. Let f be a real-valued 2-D signal. the 2-D *quaternion analytic signal* is defined as[6]

$$f_A^q(x,y) = f(x,y) + \mathbf{i} f_{\mathcal{H}_x}(x,y) + \mathbf{j} f_{\mathcal{H}_y}(x,y) + \mathbf{k} f_{\mathcal{H}_{xy}}(x,y)$$

where

$$f_{\mathcal{H}_x}(x,y) = f(x,y) \ast\ast \frac{\delta(y)}{\pi x},$$

$$f_{\mathcal{H}_y}(x,y) = f(x,y) \ast\ast \frac{\delta(x)}{\pi y},$$

$$f_{\mathcal{H}_{xy}}(x,y) = f(x,y) \ast\ast \frac{1}{\pi^2 xy}.$$

[5] `http://dsp.rice.edu/software/qwt`

[6] We have changed the notation slightly for consistency with previous results.

The function $f_{\mathcal{H}_{xy}}(\cdot)$ is the total Hilbert transform and $f_{\mathcal{H}_x}(\cdot)$ and $f_{\mathcal{H}_y}(\cdot)$ are the partial Hilbert transforms; $\delta(x)$ and $\delta(y)$ are impulse sheets along the y and x axes respectively and $**$ denotes 2-D convolution.

Per Bow (2002, p. 422), "An impulse sheet is defined such that it has an infinite length in one direction and its cross-section has the usual δ-function properties". This definition is not worded very well, but what it means is that the impulse sheet $\delta(x)$ above is a sheet in the x–y plane whose cross-section anywhere parallel to the y–z plane is a δ-function; and similarly, $\delta(y)$ is a sheet in the x–y plane whose cross-section anywhere parallel to the x–z plane is a δ-function.

This QWT is constructed by simply arranging the four components of a 2-D complex wavelet as a quaternion, using appropriate filters for the calculation of the coefficients. The basis functions are shifted and scaled copies of the following; the superscripts H, V and D label the horizontal, vertical and diagonal sub-bands respectively:

$$\begin{aligned}
f^q_{A_0}(x,y) = \quad & \phi(x,y) = \phi_h(x)\phi_h(y) + \mathbf{i}\phi_h(x)\phi_g(y) + \mathbf{j}\phi_g(x)\phi_h(y) + \mathbf{k}\phi_g(x)\phi_g(y) \\
f^q_{A_1}(x,y) = \psi^H(x,y) &= \psi_h(x)\phi_h(y) + \mathbf{i}\psi_h(x)\phi_g(y) + \mathbf{j}\psi_g(x)\phi_h(y) + \mathbf{k}\psi_g(x)\phi_g(y) \\
f^q_{A_2}(x,y) = \psi^V(x,y) &= \phi_h(x)\psi_h(y) + \mathbf{i}\phi_h(x)\psi_g(y) + \mathbf{j}\phi_g(x)\psi_h(y) + \mathbf{k}\phi_g(x)\psi_g(y) \\
f^q_{A_3}(x,y) = \psi^D(x,y) &= \psi_h(x)\psi_h(y) + \mathbf{i}\psi_h(x)\psi_g(y) + \mathbf{j}\psi_g(x)\psi_h(y) + \mathbf{k}\psi_g(x)\psi_g(y)
\end{aligned} \tag{11}$$

Chan *et al.*'s QWT function has four arguments: the image to be analysed, the level of analysis required J and four pairs of filter coefficients, two pairs `Faf`{1} `Lo` and `Hi` and `Faf`{2} `Lo` and `Hi` for the first level and two pairs `af`{1} `Lo` and `Hi` and `af`{2} `Lo` and `Hi` for subsequent levels. It returns the wavelet coefficients for each of levels 1 to J and the scaling coefficients at level $J+1$.

The way this function works is to use one filter on each column and downsample the columns by two and then use another filter on each row and downsample the rows by two.

For the four scalar terms in equations (11), `Faf`{1} (`af`{1} from level 2 onwards) filters are used in the order $\texttt{Lo}_1\texttt{-Lo}_1$, $\texttt{Lo}_1\texttt{-Hi}_1$, $\texttt{Hi}_1\texttt{-Lo}_1$, $\texttt{Hi}_1\texttt{-Hi}_1$.

The **i**-terms use `Faf`{1} and `Faf`{2} (`af`{1} and `af`{2} from level 2 onwards) respectively in the order $\texttt{Lo}_1\texttt{-Lo}_2$, $\texttt{Lo}_1\texttt{-Hi}_2$, $\texttt{Hi}_1\texttt{-Lo}_2$, $\texttt{Hi}_1\texttt{-Hi}_2$, the subscript indicating the source of the filter.

The **j**-terms use `Faf`{2} and `Faf`{1} (`af`{2} and `af`{1} from level 2 onwards) respectively in the order $\texttt{Lo}_2\texttt{-Lo}_1$, $\texttt{Lo}_2\texttt{-Hi}_1$, $\texttt{Hi}_2\texttt{-Lo}_1$, $\texttt{Hi}_2\texttt{-Hi}_1$.

The **k**-terms use `Faf`{2} (`af`{2} from level 2 onwards) respectively in the order $\texttt{Lo}_2\texttt{-Lo}_2$, $\texttt{Lo}_2\texttt{-Hi}_2$, $\texttt{Hi}_2\texttt{-Lo}_2$, $\texttt{Hi}_2\texttt{-Hi}_2$.

Chan *et al.* do not actually mention anything in their articles about the filters they used, although they do say in the comments on their code that the `Faf` filters are "Farras filters organized for the dual-tree complex DWT" and that the `af` filters are "Kingsbury Q-shift filters for the dual-tree complex DWT". Each one consists of 10 coefficients, including a few zeros.

Xu et al. (2010) "traced the evolution of the QWT", from Bülow's quaternionic Gabor filter via Bayro-Corrochano's QWT to Chan *et al.*'s QWT. They considered some potential applications in: image registration using a windowed quaternion Fourier transform; image fusion using Chan *et al.*'s QWT; and colour image recognition using quaternionic Gabor filters.

4.5. Other novel QWTs

He and Yu (2004) studied the theory of continuous wavelet transforms on the space of square-integrable quaternion-valued functions. Their QWT looks very much like the real/complex one in equation (4), except with a quaternion-valued function and wavelet.

Peng and Zhao (2004) succeeded in designing three symmetric quaternion scaling filters but as shown by Ginzberg (2013, *pp.* 130/1), these filters were in fact trivial, meaning that they could be decomposed into independent complex

Table 1: Summary of research by application which has used the QWT formulation of Chan et al. (2008).

Application	Research articles
Image disparity and optical flow	Chan et al. (2008), Wang et al. (2011), Wang et al. (2013), Kumar et al. (2014)
Edge geometry	Chan et al. (2008)
Texture recognition	Soulard and Carré (2010a), Sathyabama et al. (2011), Sathyabama (2011), Soulard and Carré (2011), Gai et al. (2013c), Li et al. (2013)
Image coding	Soulard and Carré (2010b)
Feature extraction and object recognition	Gai et al. (2011), Li et al. (2012), Gai et al. (2013b), Gai et al. (2013a), Greenblatt et al. (2013), Priyadharshini and Arivazhagan (2014), Sangeetha et al. (2014), Katunin (2014), Shen et al. (2014), Mosquera-Lopez et al. (2014), Gai and Luo (2014)
Speckle reduction	Jin et al. (2012), Liu et al. (2012a), Wu et al. (2013)
Image denoising	Yin et al. (2012), Kadiri et al. (2012), Kadiri et al. (2014), Gai et al. (2014), Yu et al. (2014), Gai and Luo (2015)
Image fusion	Liu et al. (2012b), Liu et al. (2013b), Liu et al. (2014), Yin et al. (2014), Geng et al. (2015)
Scale saliency	Le Ngo et al. (2013a), Le Ngo et al. (2013b)
Image metrics	Liu et al. (2013a), Traoré et al. (2014), Traoré et al. (2015)
Watermarking	Lei et al. (2014), Lei et al. (2015)

or real filters.

Shi (2005, *pp.* 49-51) developed a Haar QWT for colour images represented as arrays of pure quaternions or *vector images*. This seems to be the earliest

QWT for such images and we explain this representation further in section 5.4. His equations did not convey exactly what we believe he meant, so we have adjusted them slightly to make them clearer. In 1-D, we start with a quaternion signal $Q(r)$ of length $2N$, say. Then for $r \in N$, we find sums and differences divided by 2:

$$Q_L(r) = \frac{Q(2r) + Q(2r-1)}{2}$$

$$Q_H(r) = \frac{Q(2r) - Q(2r-1)}{2}.$$

In wavelet terminology, $Q_L(r)$ is the approximation and $Q_H(r)$ is the detail. If N is a power of 2, this can be repeated with $Q_L(r)$ as the signal, and so on. Finding the sums and differences of pairs of pixels along the rows and columns of a quaternion colour image would hence implement a 2-D Haar QWT.

For perfect reconstruction in 1-D, we have

$$Q(2r) = Q_L(r) + Q_H(r)$$

$$Q(2r-1) = Q_L(r) - Q_H(r),$$

which is easily extended to 2-D. As Shi admits, his 2-D "QWT" would be equivalent to three separate monochrome 2-D DWTs and would not therefore be truly quaternionic.

Carré and Denis (2006) also thought of trying to develop a QWT for use with vector images. They considered the two-channel filter bank with perfect reconstruction in Fig. 2, but with quaternion input and output and quaternion coefficients. They found that the conditions on the filters for perfect reconstruction are exactly the same as for filter banks with real coefficients, except that the order of the elements is important. The only example they tried was a Shannon QWT, for which the filter coefficients turned out to be real. This was a conference paper and there does not appear to have been a follow-up journal

paper.

Zhao and Peng (2007) define a continuous quaternion wavelet $\psi \in L^2(\mathbb{R}^2, \mathbb{H})$ as

$$\psi_{a,\theta,\boldsymbol{b}}(\boldsymbol{x}) = a^{-1}\psi\left(a^{-1}r_{-\theta}(\boldsymbol{x}-\boldsymbol{b})\right)$$

where $$r_{-\theta}(\boldsymbol{x}) = (x_1\cos(\theta) - x_2\sin(\theta), x_1\sin(\theta) + x_2\cos(\theta)),$$

$$0 \leqslant \theta \leqslant 2\pi, \quad a > 0, \quad \boldsymbol{b} \in \mathbb{R}^2.$$

They then define their QWT as

$$W_\psi : L^2\left(\mathbb{R}^2, \mathbb{H}\right) \to L^2\left(IG(2), \mathbb{H}, a^{-3}\mathrm{d}a\mathrm{d}\theta\mathrm{d}\boldsymbol{b}\right)$$

$$f(\boldsymbol{x}) \mapsto W_\psi(a,\theta,\boldsymbol{b}) = C_\psi^{-\frac{1}{2}}\langle\psi_{a,\theta,\boldsymbol{b}}, f\rangle$$

$$= C_\psi^{-\frac{1}{2}}\int_{\mathbb{R}^2}\overline{\psi_{a,\theta,\boldsymbol{b}}(\boldsymbol{x})}f(\boldsymbol{x})\mathrm{d}\boldsymbol{x}, \qquad (12)$$

where

$$IG(2) = \left\{(a, r_\theta, \boldsymbol{b}), a > 0, \theta \in [0, 2\pi], \boldsymbol{b} \in \mathbb{R}^2\right\} \quad \text{and} \quad C_\psi = \int_{\mathbb{R}^2}\frac{|\hat{\psi}(\xi)|^2}{|\xi|^2}\mathrm{d}\xi.$$

Thus the signal is decomposed by rotated as well as scaled and translated copies of the mother wavelet. This vector QWT will be recognised as one possible generalisation of that in equation (4) to more than one dimension. This QWT apparently first appeared in Zhao and Peng (2001).

Bahri et al. (2011) define their 2-D continuous QWT as:

$$T_\psi : L^2\left(\mathbb{R}^2, \mathbb{H}\right) \to L^2\left(\mathbb{R}^2, \mathbb{H}\right)$$

$$f \mapsto T_\psi f(a,\theta,\boldsymbol{b}) = \langle f, \psi_{a,\theta,\boldsymbol{b}}\rangle_{L^2(\mathbb{R}^2,\mathbb{H})}$$

$$= \int_{\mathbb{R}^2} f(\boldsymbol{x})\frac{1}{a}\overline{\psi\left(r_{-\theta}\left(\frac{\boldsymbol{x}-\boldsymbol{b}}{a}\right)\right)}\mathrm{d}\boldsymbol{x}, \qquad (13)$$

where

$$r_{-\theta}(\boldsymbol{z}) = (z_1\cos(\theta) + z_2\sin(\theta), -z_1\sin(\theta) + z_2\cos(\theta))\,, \qquad 0 \leqslant \theta \leqslant 2\pi.$$

This QWT at first sight appears to be very similar to Zhao and Peng's in equation (12): the differences are that Bahri *et al.* have the opposite sign of θ compared with Zhao and Peng, so that in the terminology used above $r_\theta(\boldsymbol{z}) = r_{-\theta}(\boldsymbol{x})$, they do not have the normalisation constant $C_\psi^{-\frac{1}{2}}$ and have the opposite order of terms in their integrand. Bahri *et al.*'s QWT is in fact completely different from Zhao and Peng's, due to the non-commutativity of quaternions. They also give an inverse transform, unlike Zhao and Peng, which takes the form of an integral w.r.t. a, θ and $\boldsymbol{b}$.

Although Bahri *et al.* do not cite Zhao and Peng (2007), they do cite Zhao and Peng (2001), which also appears in the references of Bahri (2011), Bahri et al. (2012) and Bahri et al. (2014). In the last of these, the authors define a quaternion Fourier transform as

$$\mathcal{F}_q[f(\boldsymbol{x})](\boldsymbol{\omega}) = \hat{f}(\boldsymbol{\omega}) = \int_{\mathbb{R}^2} f(\boldsymbol{x})\exp(-\boldsymbol{\mu}[\boldsymbol{\omega}\cdot\boldsymbol{x}])\mathrm{d}\boldsymbol{x},$$

where $\boldsymbol{\mu} = (\mathbf{i}+\mathbf{j}+\mathbf{k})/\sqrt{3}$. They then use this to rewrite equation (13) as

$$T_\psi f(a,\theta,\boldsymbol{b}) = \frac{1}{(2\pi)^2}\int_{\mathbb{R}^2} a\hat{f}(\boldsymbol{\omega})\exp(-\boldsymbol{\mu}[\boldsymbol{\omega}\cdot\boldsymbol{b}])\overline{\hat{\psi}(ar_{-\theta}(\boldsymbol{\omega}))}\mathrm{d}\boldsymbol{\omega}.$$

They go on to establish some theorems involving this formulation of their 2-D QWT.

A signal with vector-valued samples can be processed using matrices as filter coefficients: this is an alternative representation of hypercomplex algebras which is mathematically more general. A convolution consists of multiplying the signal samples (vectors) by the filter coefficients (matrices of compatible dimension), yielding modified signal samples (vectors). Given this way of rep-

resenting and thinking about vector signal processing, it is natural to consider wavelet transforms with matrix coefficients. Xia and Suter (1996) introduced vector-valued wavelets, as they called them, for the analysis of vector-valued signals. Their MRA is similar to that in subsection 2.5, except that $L^2(\mathbb{R})$ is replaced by $L^2(\mathbb{R}, \mathbb{C}^{N\times N})$. Matrix valued wavelets (MVAs), as they are most commonly called, have since been studied in their own right. He and Yu (2005) appear to have been the first to consider quaternion MVWs and an associated quaternion-valued MRA analysis, using the 2×2 complex matrix representation of quaternions. However, they tried to design filters in the frequency domain and forgot the noncommutativity of matrix multiplication per Ginzberg (2013), resulting in their method only working for trivial scaling and wavelet filters. Bahri (2010) did something very similar to He and Yu with 2×2 complex matrices and did not notice a similar noncommutativity problem, also per Ginzberg (2013).

Ginzberg and Walden (2013) constructed some novel families of non-trivial 2×2 and 4×4 MVWs. As per Ginzberg (2013, p. 122), "We define an $n\times n$ MVW to be trivial if it can be decomposed into independent lower-dimensional MVWs (in some appropriate orthogonal basis of $\mathbb{R}^n$). Every MVW is then composed of one or more non-trivial MVWs". They went on to construct a 4×4 non-trivial symmetric quaternion wavelet with compact support, specifically a length 10 Daubechies quaternion scaling filter together with the corresponding wavelet filter. Daubechies wavelets are characterised by maximal vanishing moments for a given length of filter: the low- and high-frequency passbands can be made as flat as one wishes by increasing the lengths of the filters. Their method of construction for the scaling filter was to derive and solve the following set of

design equations:

$$\sum_{k=0}^{9} \boldsymbol{H}_k = \sqrt{2}\,\boldsymbol{I}_4,$$

$$\sum_{k=0}^{9} (-1)^k\, k^d\, \boldsymbol{H}_k = \boldsymbol{0}_4 \qquad \text{for} \qquad d = 0 \ldots 4,$$

$$\sum_{k=0}^{8-2m} \boldsymbol{H}_k\, \boldsymbol{H}_{k+2m}^T = \delta_{m,0}\, \boldsymbol{I}_4 \qquad \text{for} \qquad m = 1 \ldots 4,$$

where the $\boldsymbol{H}_k$ were each 4×4 matrix representations of quaternions with four unknowns appearing four times.

The solutions of these equations in terms of the equivalent quaternions are:

$$\boldsymbol{h}_0 = \boldsymbol{h}_9 = \frac{\sqrt{35}}{256}\mathbf{i},$$

$$\boldsymbol{h}_1 = \boldsymbol{h}_8 = \frac{1}{256}\left(-5\sqrt{2} + \sqrt{35}\,\mathbf{k}\right)$$

$$\boldsymbol{h}_2 = \boldsymbol{h}_7 = \frac{1}{256}\left(-7\sqrt{2} - 7\sqrt{35}\,\mathbf{i} + 3\sqrt{35}\,\mathbf{k}\right)$$

$$\boldsymbol{h}_3 = \boldsymbol{h}_6 = \frac{1}{256}\left(35\sqrt{2} - 5\sqrt{35}\,\mathbf{i} + \sqrt{35}\,\mathbf{k}\right)$$

$$\boldsymbol{h}_4 = \boldsymbol{h}_5 = \frac{1}{256}\left(105\sqrt{2} + 11\sqrt{35}\,\mathbf{i} - 5\sqrt{35}\,\mathbf{k}\right).$$

Ginzberg then used a function he wrote using functions from the `mw` toolbox for MATLAB® by Keinert (2004) to find the corresponding wavelet filter coef-

ficients as:

$$\boldsymbol{g}_0 = -\boldsymbol{g}_9 = \frac{1}{24576}\left(89\sqrt{35}\,\mathbf{i} + 35\sqrt{2}\,\mathbf{j} - 35\sqrt{35}\,\mathbf{k}\right)$$

$$\boldsymbol{g}_1 = -\boldsymbol{g}_8 = \frac{1}{24576}\left(-480\sqrt{2} + 35\sqrt{35}\,\mathbf{i} - 175\sqrt{2}\,\mathbf{j} + 79\sqrt{35}\mathbf{k}\right)$$

$$\boldsymbol{g}_2 = -\boldsymbol{g}_7 = \frac{1}{3072}\left(84\sqrt{2} - 91\sqrt{35}\,\mathbf{i} + 35\sqrt{2}\,\mathbf{j} + \sqrt{35}\,\mathbf{k}\right)$$

$$\boldsymbol{g}_3 = -\boldsymbol{g}_6 = \frac{1}{256}\left(35\sqrt{2} + 5\sqrt{35}\,\mathbf{i} - \sqrt{35}\,\mathbf{k}\right)$$

$$\boldsymbol{g}_4 = -\boldsymbol{g}_5 = \frac{1}{12288}\left(-5040\sqrt{2} + 577\sqrt{35}\,\mathbf{i} - 245\sqrt{2}\,\mathbf{j} + 5\sqrt{35}\,\mathbf{k}\right).$$

In the above equations we have swapped Ginzberg's $\boldsymbol{G}$'s with $\boldsymbol{H}$'s and $\boldsymbol{g}$'s with $\boldsymbol{h}$'s to match our convention of using H for low-pass filters and G for high-pass filters.

This is as far as Ginzberg took his QWT: he only found the filter coefficients for the analysis side of a quaternion QMF, but not those for the synthesis side.

Guo et al. (2012) define their quaternion curvelet transform in virtually the same way as Bahri *et al.* define their 2-D QWT and use it in colour image fusion. They recognise that treating the R, G and B channels holistically as described in section 5.4 reduces blur, preserving the greatest amount of colour information, and use colour images represented as pure quaternions but do not describe exactly how they evaluate their transform. However, Pang et al. (2012), which has two authors in common with Guo et al. (2012), do explain how their QWTs are computed. They use low- and high-pass decomposition filters ϕ_d and φ_d and low- and high-pass reconstruction filters ϕ_r and φ_r, which they define

as:

$$\phi_d = \begin{bmatrix}0.0000 & -0.1768 & 0.3536 & 1.0607 & 0.3536 & -0.1768\end{bmatrix} \exp(\boldsymbol{\mu}\pi/4),$$
$$\varphi_d = \begin{bmatrix}0.0000 & 0.3536 & -0.7071 & 0.3536 & 0.0000 & 0.0000\end{bmatrix} \exp(\boldsymbol{\mu}\pi/4),$$
$$\phi_r = \begin{bmatrix}0.0000 & 0.3536 & 0.7071 & 0.3536 & 0.0000 & 0.0000\end{bmatrix} \exp(\boldsymbol{\mu}\pi/4),$$
$$\varphi_r = \begin{bmatrix}0.0000 & 0.1768 & 0.3536 & -1.0607 & 0.3536 & 0.1768\end{bmatrix} \exp(\boldsymbol{\mu}\pi/4),$$

where $\boldsymbol{\mu} = (\mathbf{i} + \mathbf{j} + \mathbf{k})/\sqrt{2}$, although presumably $\sqrt{2}$ should read $\sqrt{3}$. Guo *et al.* do not explain where these filter coefficients come from. They report an improvement on previous methods of colour image fusion.

Hogan and Morris (2012) developed some theory for quaternionic signals using the Clifford-Fourier transform of Brackx et al. (2006) for $C\ell(0,2)$, which is a quaternion Fourier transform (QFT). They used this QFT in the proof of a quaternionic analogue of the QMF condition: a quaternionic orthonormal scaling function must necessarily satisfy this. They went on to find conditions to be satisfied by the corresponding quaternion wavelet functions. These conditions can be expressed as a matrix equation and they found an equivalent system of quadratic equations that it would be possible to solve numerically. They then found conditions that would be sufficient to guarantee a quaternion scaling function would have compact support. They were not, however, able to actually construct a quaternion wavelet basis from a QFT series and conclude that their theory must be incomplete. They were, however, able to construct a quaternionic biorthogonal wavelet basis and give an example of such a wavelet basis and illustrate the resulting wavelets. Much of this article also appeared, in a slightly expanded form, in Morris (2014, *pp.* 63-121).

4.6. The monogenic approach

In this section we have so far confined ourselves just to QWTs that were so-named by those who introduced them. Although not "officially" QWTs,

monogenic wavelet transforms (MWTs) are related and therefore warrant a brief mention.

Olhede and Metikas (2009) devised a 2-D version of the 1-D analytic wavelet, using the work of Chan et al. (2004a) and the dual-tree ℂWT of Selesnick et al. (2005), and named it the "monogenic wavelet". This involved generalising the 1-D analytic signal to the 2-D *monogenic signal* (see *e.g.*, Felsberg and Sommer (2001)). Olhede and Metikas defined the monogenic extension of any real-valued mother wavelet $\psi(\boldsymbol{x})$ as

$$\psi^{+}(\boldsymbol{x}) = \mathcal{M}\psi(\boldsymbol{x}) = \psi(\boldsymbol{x}) + \mathcal{R}\psi(\boldsymbol{x}) = \psi(\boldsymbol{x}) + \left(\mathbf{i}\psi^{(1)}(\boldsymbol{x}) + \mathbf{j}\psi^{(2)}(\boldsymbol{x})\right),$$

where $\psi^{(1)} = \mathcal{R}_1\psi$, $\psi^{(2)} = \mathcal{R}_2\psi$ and $\mathcal{R}$ is the Riesz transform; the $\mathbf{i}$ and $\mathbf{j}$ are two of the three quaternion basis elements. They went on to study variations of this wavelet and the associated MWTs. These MWTs were intended for use with monochrome images. Along the same lines, Unser et al. (2009) used two parallel filter banks to implement multiresolution monogenic analysis.

Soulard and Carré have made a number of contributions to this area in recent years, extending the monogenic idea to colour images. In Soulard et al. (2013) they define their tensor-based colour MWT for each scale i as

$$c_M(\boldsymbol{k}) = \left[c^{\mathsf{R}}_{i,k}, c^{\mathsf{G}}_{i,k}, c^{\mathsf{B}}_{i,k}, \mathcal{N}_{i,k}\right],$$

where

$$c^{\mathsf{C}}_{i,k} = \left(\psi_i * s^{\mathsf{C}}\right)\left(2^{-(i+1)}\mathbf{k}\right) \qquad \text{and} \qquad d^{\mathsf{C}}_{i,k} = \left(\mathcal{R}\left(\psi_i * s^{\mathsf{C}}\right)\right)\left(2^{-(i+1)}\mathbf{k}\right)$$

with signal s, $\mathsf{C} \in \{\mathsf{R}, \mathsf{G}, \mathsf{B}\}$ and $\mathcal{N}_{i,k} = \sqrt{\left|d^{\mathsf{R}}_{i,k}\right|^2 + \left|d^{\mathsf{G}}_{i,k}\right|^2 + \left|d^{\mathsf{B}}_{i,k}\right|^2}$.

The monogenic approach actually offers the potential for generalisation to more than four dimensions, whereas QWTs are limited to four.

5. Discussion

We have seen in the previous sections, several possible approaches to wavelet transforms for quaternionic (*i.e.*, not real-valued) signals and we now consider the ramifications of these ideas and how they relate to each other. We also consider how classical filter theory can be extended to complex and vector-valued wavelets and this leads us to the question of what makes a truly quaternionic wavelet.

5.1. Short Time Fourier Transform approaches

The STFT approach developed from Gabor's ideas is a form of wavelet transform, but it is based on Fourier transforms, which use sinusoidal basis functions. This type of wavelet transform is not based on basis functions with finite support. As we have seen, there are wavelet transforms based on wavelets which do have finite support and we make a distinction between the two in what follows.

It is not surprising that the STFT-based approach to defining wavelet transforms has been adopted by many researchers to provide quaternion STFT/wavelet transforms. The Fourier transforms needed already existed (including numerical implementations) and the use of Gaussian or other window functions presented no problems because they are real-valued.

5.2. Generalising classical wavelets

Turning to the more difficult problem of generalising classical wavelet transforms based on wavelets with finite support (*e.g.*, Haar, Daubechies), there are significant research questions still to be studied. This can be seen even in the complex case. Putting aside the dual-tree approaches to wavelets as not being truly complex, let us consider the complex case in some detail, partly for its own sake, and partly because it provides a simpler model to work with initially than the quaternions. Consider a complex signal and a truly complex discrete

wavelet transform. Referring to Fig. 2, an immediate problem is how to define analysis and synthesis filters which process complex signals (and which therefore presumably must have complex filter coefficients). We do not know of any significant theoretical work done on the concept of *frequency response* for such filters, let alone design methods, nor on the frequency content of a signal. As an example of the problems here, consider how the classical Fourier transform represents a real signal using positive and negative frequency complex exponentials, whose imaginary parts cancel out. What is a negative frequency? In the real case it appears to be a mathematical artefact due to the use of complex exponentials, but in the complex case it is simply explained: a negative frequency exponential rotates in the complex plane in the negative sense (that is clockwise, by mathematical convention), whereas a positive frequency exponential rotates in the positive sense. Now, a complex signal can clearly have both positive and negative frequency content (being composed of exponentials rotating in either sense) and a Fourier transform of a complex signal will, in general, have no conjugate symmetry, unlike the real case. We believe that the concept of frequency response needs to represent the response of a filter to positive and negative frequencies independently.

5.3. Filter theory, etc

Noting that there is a gap in knowledge in the area of complex filter theory, we then note that the same gap occurs with vector-valued signals, whether represented by quaternions or by vectors in the linear algebra sense or by elements of other hypercomplex algebras. We know that oscillation at a single frequency in a vector-valued signal is confined to a planar ellipse, regardless of the dimensionality of the vector space (Sangwine, 2016), but we do not know how to design filters to handle such signals, even for such apparently simple tasks as separation of oscillations in different planes or in different senses of rotation

(polarization). The problem becomes even harder if we consider a modulated ellipse, as described by Lilly (2011). We have seen in section 4.5 that Carré and Denis attempted to generalise the classical QMF representation of a DWT to a QWT by using filter banks with quaternion-valued coefficients, but did not actually demonstrate a filter with quaternion coefficients. Ginzberg and Walden overcame the problem by using the matrix representation of quaternions.

5.4. What makes a QWT truly quaternionic?

The majority of the QWTs we have looked at could have been implemented using DWTs or ℂWTs without reference to quaternions, so should these ones really be called QWTs? Alfsmann et al. (2007) give the main reason for the use of hypercomplex algebras in signal processing:

> The holistic, compact processing of vector-valued signals that are a function of one or more independent parameters (*e.g.*, time, location, physical quantities). Here, the dimension of the algebra must be chosen in compliance with the dimension of the signal vector. This means that each vector-sample is treated as a whole rather than treating its components separately. Classically, the reason for this is that *the sample as a whole conveys information (direction in vector space) that is lost if the components of the sample are processed independently.* [our emphasis].

We contend that the "quaternion" in "QWT" should refer to a (pure or full) quaternion-valued signal. In colour image processing this would mean that the proportions of the three primary colours of each pixel would be the factors multiplying a quaternion's three imaginary parts. In RGB colour space, these would be the co-ordinates of the end of each pixel's colour vector. This representation would thus not lose the potentially useful information that might be contained in the correlation between different primary colours in an individual pixel.

Instead of treating each primary colour separately as illustrated diagrammatically in Fig. 9a, a *true* QWT should treat each pixel holistically rather as in Fig. 9b, where each of R', G' and B' depends on all of R, G and B. This is what the quaternion Fourier transform of Ell and Sangwine (2007) achieves.

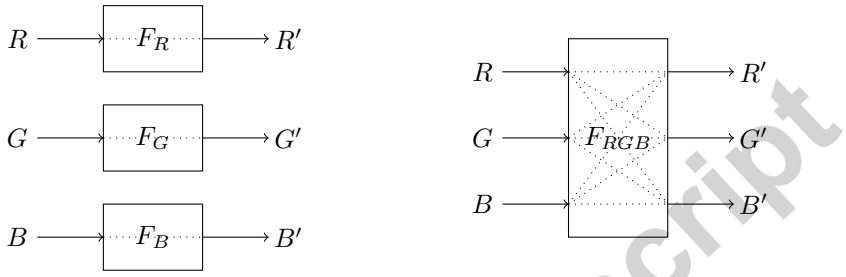

(a) Colour image processing with each primary colour processed separately.

(b) Processing of colour images represented as quaternions.

Figure 9: Diagrams illustrating the essential difference between "conventional" colour image processing and with quaternion or vector images.

6. Conclusion

We have seen how real discrete wavelet transforms (DWTs) came about and how dual-tree complex wavelet transforms (ℂWTs) were introduced to try to overcome the problems of the former, namely oscillations around discontinuities, shift variance, aliasing and lack of directionality. We saw then that the original so-called quaternion wavelet transforms (QWTs) were really DWTs or ℂWTs in disguise: they had real filter coefficients and were designed for real signals. As such, they would not cope with quaternion signals and to call them QWTs was, in our opinion, technically incorrect. In recent years, a few researchers have envisioned the development of a true QWT, one that was not equivalent to several separate DWTs or ℂWTs in parallel. In particular, Carré and Denis (2006) apparently understood the problem, but their QWT had real filter coefficients and so was equivalent to three separate DWTs; Hogan and Morris (2012) had some success with implementing a biorthogonal QWT which was truly quater-

nionic; and Ginzberg and Walden (2013) and Ginzberg (2013) introduced a true quaternion matrix valued wavelet, which has the significant advantage of being based on well-known matrix algebra.

References

D. Alfsmann, H. G. Göckler, S. J. Sangwine, and T. A. Ell. Hypercomplex algebras in digital signal processing: Benefits and drawbacks. In *Proceedings of the 15th European Signal Processing Conference (EUSIPCO 2007) held in Poznań, Poland*, pages 1322–1326. IEEE, 2007. Link: `http://www.eurasip.org/Proceedings/Eusipco/Eusipco2007/Papers/c2l-b01.pdf`.

M. Bahri. Construction of quaternion-valued wavelets. *Matematika*, 26(1):107–114, 2010. Link: `http://www.matematika.utm.my/index.php/matematika/article/view/553/546`.

M. Bahri. Quaternion algebra-valued wavelet transform. *Applied Mathematical Sciences*, 5(71):3531–3540, 2011. Link: `http://www.m-hikari.com/ams/ams-2011/ams-69-72-2011/bahriAMS69-72-2011.pdf`.

M. Bahri, R. Ashino, and R. Vaillancourt. Two-dimensional quaternion wavelet transform. *Applied Mathematics and Computation*, 218(1):10–21, 2011. DOI: `10.1016/j.amc.2011.05.030`.

M. Bahri, R. Ashino, and R. Vaillancourt. Two-dimensional quaternion Fourier transform of type II and quaternion wavelet transform. In *Proceedings of the 2012 International Conference on Wavelet Analysis and Pattern Recognition (ICWAPR 2012), held in Xian, China*, pages 359–364. IEEE, 2012. DOI: `10.1109/ICWAPR.2012.6294808`.

M. Bahri, R. Ashino, and R. Vaillancourt. Continuous quaternion Fourier and wavelet transforms. *International Journal of Wavelets, Multiresolution and*

Information Processing, 12(4), 2014. Article no. 1460003, DOI: 10.1142/S0219691314600030.

E. Bayro-Corrochano. Multi–resolution image analysis using the quaternion wavelet transform. *Numerical Algorithms*, 39(1–3):35–55, 2005. DOI: 10.1007/s11075-004-3619-8.

E. Bayro-Corrochano. The theory and use of the quaternion wavelet transform. *Journal of Mathematical Imaging and Vision*, 24(1):19–35, 2006. DOI: 10.1007/s10851-005-3605-3.

E. Bayro-Corrochano and M. de La Torre Gomora. Image processing using the quaternion wavelet transform. In *Progress in Pattern Recognition, Image Analysis and Applications: Proceedings of the 9th IberoAmerican Congress on Pattern Recognition (CIARP 2004), held in Puebla, Mexico*, volume 3287 of *Lecture Notes in Computer Science*, pages 613–620. Springer Berlin Heidelberg, 2004. DOI: 10.1007/978-3-540-30463-0_77.

C. Blatter. *Wavelets: A Primer*. A. K. Peters, Natick, MA, 1998. Not available online.

S.-T. Bow. *Pattern Recognition and Image Preprocessing*. Signal Processing and Communications. Marcel Dekker, New York, 2nd edition, 2002. Link: http://www.crcnetbase.com/isbn/9780203903896.

F. Brackx, N. D. Schepper, and F. Sommen. The two-dimensional Clifford–Fourier transform. *Journal of Mathematical Imaging and Vision*, 26(1–2): 5–18, 2006. DOI: 10.1007/s10851-006-3605-y.

T. Bülow. *Hypercomplex Spectral Signal Representations for the Processing and Analysis of Images*. PhD thesis, Institut für Informatik und Praktische Mathe-

matik der Christian-Albrechts-Universität, Kiel, Germany, 1999. Link: http://www.uni-kiel.de/journals/receive/jportal_jparticle_00000190.

P. Carré and P. Denis. Quaternionic wavelet transform for colour images. In *Proceedings of SPIE: Wavelet Applications in Industrial Processing IV, held in Boston, MA*, volume 6383. SPIE - The International Society for Optical Engineering, 2006. Article no. 638301, DOI: 10.1117/12.685942.

W. L. Chan, H. Choi, and R. Baraniuk. Quaternion wavelets for image analysis and processing. In *Proceedings of the 2004 IEEE International Conference on Image Processing (ICIP 2004), held in Singapore*, volume 5, pages 3057–3060. IEEE, 2004a. DOI: 10.1109/ICIP.2004.1421758.

W. L. Chan, H. Choi, and R. Baraniuk. Directional hypercomplex wavelets for multidimensional signal analysis and processing. In *Proceedings of the 2004 IEEE International Conference on Acoustics, Speech and Signal Processing (ICASSP 2004), held in Montreal, Canada*, volume III, pages 996–999. IEEE, 2004b. DOI: 10.1109/ICASSP.2004.1326715.

W. L. Chan, H. Choi, and R. Baraniuk. Coherent image processing using quaternion wavelets. In *Proceedings of SPIE: Wavelets XI, held in San Diego, CA*, volume 5914. SPIE, 2005. Article no. 59140Z, DOI: 10.1117/12.615393.

W. L. Chan, H. Choi, and R. G. Baranuik. Multiscale image disparity estimation using the quaternion wavelet transform. In *Proceedings of the 2006 IEEE International Conference on Image Processing (ICIP 2006), held in Atlanta, Georgia*, pages 1229–1232. IEEE, 2006. DOI: 10.1109/ICIP.2006.312547.

W. L. Chan, H. Choi, and R. G. Baraniuk. Coherent multiscale image processing using dual-tree quaternion wavelets. *IEEE Transactions on Image Processing*, 17(7):1069–1082, 2008. DOI: 10.1109/TIP.2008.924282.

Q. Chen, Y. Xu, C. Li, N. Liu, and X. Yang. An image quality assessment metric based on quaternion wavelet transform. In *Proceedings of the 2013 IEEE International Conference on Multimedia and Expo Workshops (ICMEW 2013), held in San Jose, California*. IEEE, 2013. DOI: 10.1109/ICMEW.2013.6618378.

C. K. Chui and J. Wang. High-order orthonormal scaling functions and wavelets give poor time-frequency localization. *Journal of Fourier Analysis and Applications*, 2(5):415–426, 1995. DOI: 10.1007/s00041-001-4035-2.

A. Cohen, I. Daubechies, and J.-C. Feauveau. Biorthogonal bases of compactly supported wavelets. *Communications on Pure and Applied Mathematics*, 45 (5):485–560, 1992. DOI: 10.1002/cpa.3160450502.

I. Daubechies. Orthonormal bases of compactly supported wavelets. *Communications on Pure and Applied Mathematics*, 41(7):909–996, 1988. DOI: 10.1002/cpa.3160410705.

I. Daubechies. *Ten Lectures on Wavelets*. CBMS-NSF Regional Conference Series in Applied Mathematics. The Society for Industrial and Applied Mathematics, Philadelphia, PA, 1992. DOI: 10.1137/1.9781611970104.

X. Ding, Y. Xu, L. Deng, and X. Yang. Colorization using quaternion algebra with automatic scribble generation. In *Advances in Multimedia Modeling: Proceedings of the 18th International Conference on Multimedia Modeling (MMM 2012) held in Klagenfurt, Austria*, volume 7131 of *Lecture Notes in Computer Science*, pages 103–114. Springer Berlin Heidelberg, 2012. DOI: 10.1007/978-3-642-27355-1_12.

T. A. Ell and S. J. Sangwine. Hypercomplex Fourier transforms of color images. *IEEE Transactions on Image Processing*, 16(1):22–35, 2007. DOI: 10.1109/TIP.2006.884955.

M. Felsberg and G. Sommer. The monogenic signal. *IEEE Transactions on Signal Processing*, 49(12):3136–3144, 2001. DOI: 10.1109/78.969520.

Z. Feng, Y. Xu, and X. Yang. Quaternion phase congruency model for edge saliency map extraction and image blur measurement. In *Proceedings of the 2014 IEEE International Symposium on Broadband Multimedia Systems and Broadcasting (BMSB 2014), held in Beijing, China*. IEEE, 2014. DOI: 10.1109/BMSB.2014.6873515.

D. Gabor. Theory of communication Part 1 - The analysis of information. *The Journal of the Institute of Electrical Engineers - Part III: Radio and Communication Engineering*, 93(26):429–441, 1946a. DOI: 10.1049/ji-3-2.1946.0074.

D. Gabor. Theory of communication Part 2 - The analysis of hearing. *The Journal of the Institute of Electrical Engineers - Part III: Radio and Communication Engineering*, 93(26):442–445, 1946b. DOI: 10.1049/ji-3-2.1946.0075.

S. Gai and L. Luo. Visual objects tracking and identification based on reduced quaternion wavelet transform. *Signal, Image and Video Processing*, 8(1 Supplement):75–84, 2014. DOI: 10.1007/s11760-014-0636-5.

S. Gai and L. Luo. Image denoising using normal inverse Gaussian model in quaternion wavelet domain. *Multimedia Tools and Applications*, 74(3):1107–1124, 2015. DOI: 10.1007/s11042-013-1812-2.

S. Gai, P. Liu, J. Liu, and X. Tang. Banknote image retrieval using rotated quaternion wavelet filters. *International Journal of Computational Intelligence Systems*, 4(2):268–276, 2011. DOI: 10.1080/18756891.2011.9727782.

S. Gai, G. Yang, and M. Wan. Employing quaternion wavelet transform for

banknote classification. *Neurocomputing*, 118:171–178, 2013a. DOI: 10.1016/j.neucom.2013.02.029.

S. Gai, G. Yang, and S. Zhang. New feature extraction approach for bank note classification using quaternion wavelets. *Journal of Intelligent and Fuzzy Systems*, 25(3):685–694, 2013b. DOI: 10.3233/IFS-120675.

S. Gai, G. Yang, and S. Zhang. Multiscale texture classification using reduced quaternion wavelet transform. *International Journal of Electronics and Communications (AEÜ)*, 67(3):233–241, 2013c. DOI: 10.1016/j.aeue.2012.08.004.

S. Gai, G. Yang, M. Wan, and L. Wang. Hidden Markov tree model of images using quaternion wavelet transform. *Computers and Electrical Engineering*, 40(3):819–832, 2014. DOI: 10.1016/j.compeleceng.2014.02.009.

P. Geng, X. Su, and T. Xu. Medical image fusion based on quaternion wavelet transform and visibility feature. *International Journal of Applied Mathematics and Machine Learning*, 2(1):9–26, 2015. Link: http://scientificadvances.co.in/admin/img_data/904/images/[2]%20IJAMML%207100121448%20Peng%20geng,%20Xing%20Su%20and%20Tan%20Xu%20[9-26].pdf.

P. Ginzberg. *Quaternion Matrices: Statistical Properties and Applications to Signal Processing and Wavelets*. PhD, Imperial College Department of Mathematics, London, UK, 2013. Link: http://hdl.handle.net/10044/1/18975.

P. Ginzberg and A. T. Walden. Matrix-valued and quaternion wavelets. *IEEE Transactions on Signal Processing*, 61(6):1357–1367, 2013. DOI: 10.1109/TSP.2012.2235434.

J. C. Goswami and A. K. Chan. *Fundamentals of Wavelets: Theory, Algorithms*

and Applications. Microwave and Optical Engineering. John Wiley and Sons, Inc, 2nd edition, 2011. DOI: 10.1002/9780470926994.

P. Goupillaud, A. Grossmann, and J. Morlet. Cycle-octave and related transforms in seismic signal analysis. *Geoexploration*, 23(1):85–102, 1984. DOI: 10.1016/0016-7142(84)90025-5.

A. Greenblatt, C. Mosquera-Lopez, and S. Agaian. Quaternion neural networks applied to prostate cancer Gleason grading. In *Proceedings of the 2013 IEEE International Conference on Systems, Man and Cybernetics (SMC 2013), held in Manchester, UK*, pages 1144–1149. IEEE, 2013. DOI: 10.1109/SMC.2013.199.

A. Grossmann and J. Morlet. Decomposition of Hardy functions into square integrable wavelets of constant shape. *SIAM Journal on Mathematical Analysis*, 15(4):723–736, 1984. DOI: 10.1137/0515056.

L. Guo, M. Dai, and M. Zhu. Multifocus color image fusion based on quaternion curvelet transform. *Optics Express*, 20(17):18846–18860, 2012. DOI: 10.1364/OE.20.018846.

A. Haar. Zur Theorie der orthogonalen Funktionensysteme. *Mathematische Annalen*, 69(3):331–371, 1910. DOI: 10.1007/BF01456326.

J. He and B. Yu. Continuous wavelet transforms on the space $L^2(\mathbb{R}, \mathbb{H}; \mathrm{d}x)$. *Applied Mathematics Letters*, 17(1):111–121, 2004. DOI: 10.1016/S0893-9659(04)90021-3.

J.-X. He and B. Yu. Wavelet analysis of quaternion–valued time–series. *International Journal of Wavelets, Multiresolution and Information Processing*, 3 (2):233–246, 2005. DOI: 10.1142/S0219691305000804.

J. A. Hogan and J. D. Lakey. Non-translation-invariance and the synchronization problem in wavelet sampling. *Acta Applicandae Mathematicae*, 107(1–3): 373–398, 2009. DOI: 10.1007/s10440-009-9480-y.

J. A. Hogan and A. J. Morris. Quaternionic wavelets. *Numerical Functional Analysis and Optimization*, 33(7-9):1031–1062, 2012. DOI: 10.1080/01630563.2012.682140.

S. Jaffard, Y.Meyer, and R. D. Ryan. *Wavelets: Tools for Science and Technology*. The Society for Industrial and Applied Mathematics, Philadelphia, PA, 2nd edition, 2001. DOI: 10.1137/1.9780898718119.

J. Jin, Y. Liu, Q. Wang, and S. Yi. Ultrasonic speckle reduction based on soft thresholding in quaternion wavelet domain. In *Proceedings of the 2012 IEEE International Conference on Instrumentation and Measurement Technology (I2MTC 2012), held in Graz, Austria*. IEEE, 2012. DOI: 10.1109/I2MTC.2012.6365367.

M. Kadiri, M. Djebbouri, and P. Carré. Image denoising using selective neighboring quaternionic wavelet coefficients. In *Proceedings of the 24th International Conference on Microelectronics (ICM 2012), held in Algiers, Algeria*. IEEE, 2012. DOI: 10.1109/ICM.2012.6471420.

M. Kadiri, M. Djebbouri, and P. Carré. Magnitude-phase of the dual-tree quaternionic wavelet transform for multispectral satellite image denoising. *EURASIP Journal on Image and Video Processing*, 41, 2014. DOI: 10.1186/1687-5281-2014-41.

A. Katunin. Identification of stiff inclusion in circular composite plate based on quaternion wavelet analysis of modal shapes. *JVE Journal of Vibroengineering*, 16(5):2545–2551, 2014. Researchgate: www.researchgate.net/publication/264790261.

F. Keinert. Multiwavelet toolbox for MATLAB®. Online, 2004. Available from: http://orion.math.iastate.edu/keinert/book.html [Last accessed 30th November 2016].

N. G. Kingsbury. The dual-tree complex wavelet transform: a new technique for shift invariance and directional filters. In *Proceedings of the 9th European Signal Processing Conference (EUSIPCO 1998), held in Rhodes, Greece*. IEEE, 1998. Link: http://ieeexplore.ieee.org/stamp/stamp.jsp?tp=&arnumber=7089719.

N. G. Kingsbury and J. F. A. Magarey. Wavelet transforms in image processing. In *Signal Analysis and Prediction*, Applied and Numerical Harmonic Analysis, chapter 2, pages 27–46. Birkhäuser Boston, 1998. DOI: 10.1007/978-1-4612-1768-8_2.

J. Kovačević, V. K. Goyal, and M. Vetterli. *Fourier and Wavelet Signal Processing*. Cambridge University Press, 2014. Available online at: http://www.fourierandwavelets.org/FWSP_a3.2_2013.pdf [last accessed 6th July 2016].

S. Kumar, S. Kumar, N. Sukavanam, and B. Raman. Dual tree fractional quaternion wavelet transform for disparity estimation. *ISA Transactions*, 53 (2):547–559, 2014. DOI: 10.1016/j.isatra.2013.12.001.

A. C. Le Ngo, K. Li-Minn Ang, G. Qiu, and J. Kah-Phooi Seng. Wavelet-based scale saliency. *ArXiv e-prints*, 2013a. arxiv.org/abs/1301.2884v1.

A. C. Le Ngo, K. Li-Minn Ang, G. Qiu, and J. Kah-Phooi Seng. Information-based scale saliency methods with wavelet sub-band energy density descriptors. In *Proceedings of the 5th Asian Conference on Intelligent Information and Database Systems (ACIIDS 2013), held in Kuala Lumpur, Malaysia*, vol-

ume 7803 of *Lecture Notes in Computer Science*, pages 366–376. Springer Berlin Heidelberg, 2013b. DOI: 10.1007/978-3-642-36543-0_38.

B. Lei, D. Ni, S. Chen, T. Wang, and F. Zhou. Optimal image watermarking scheme based on chaotic map and quaternion wavelet transform. *Nonlinear Dynamics*, 78(4):2897–2907, 2014. DOI: 10.1007/s11071-014-1634-4.

B. Lei, F. Zhou, E.-L. Tan, D. Ni, H. Lei, S. Chen, and T. Wang. Optimal and secure audio watermarking scheme based on self-adaptive particle swarm optimization and quaternion wavelet transform. *Signal Processing*, 113:80–94, 2015. DOI: 10.1016/j.sigpro.2014.11.007.

P. Lévy. *Processus Stochastiques et Mouvement Brownien*. Gautier-Villars, Paris, 1948. Not available online.

C. Li, J. Li, and B. Fu. Magnitude-phase of quaternion wavelet transform for texture representation using multilevel copula. *IEEE Signal Processing Letters*, 20(8):799–802, 2013. DOI: 10.1109/LSP.2013.2247596.

C.-R. Li, J.-P. Li, X.-C. Yang, and Z.-W. Liang. Gait recognition using the magnitude and phase of quaternion wavelet transform. In *Proceedings of the 2012 International Conference on Wavelet Active Media Technology and Information Processing (ICWAMTIP 2012), held in Chengdu, China*, pages 322–324. IEEE, 2012. DOI: 10.1109/ICWAMTIP.2012.6413504.

J. M. Lilly. Modulated oscillations in three dimensions. *IEEE Transactions on Image Processing*, 59(12):5930–5943, 2011. DOI: 10.1109/TSP.2011.2164914.

Y. Liu, J. Jin, Q. Wang, and Y. Shen. Phase-preserving speckle reduction based on soft thresholding in quaternion wavelet domain. *Journal of Elec-*

tronic Imaging, 21(4), 2012a. Article no. 043009, DOI: 10.1117/1.JEI.21.4.043009.

Y. Liu, J. Jin, Q. Wang, and S. Yi. Ultrasound extended-field-of-view imaging based on motion estimation using quaternion wavelet. In *Proceedings of the 2012 IEEE International Conference on Instrumentation and Measurement Technology (I2MTC 2012), held in Graz, Austria*. IEEE, 2012b. DOI: 10.1109/I2MTC.2012.6365366.

Y. Liu, J. Jin, Q. Wang, and Y. Shen. Phases measure of image sharpness based on quaternion wavelet. *Pattern Recognition Letters*, 34(9):1063–1070, 2013a. DOI: 10.1016/j.patrec.2013.03.002.

Y. Liu, J. Jin, Q. Wang, Y. Shen, and X. Dong. Novel focus region detection method for multifocus image fusion using quaternion wavelet. *Journal of Electronic Imaging*, 22(2), 2013b. Article no. 023017, DOI: 10.1117/1.JEI.22.2.023017.

Y. Liu, J. Jin, Q. Wang, Y. Shen, and X. Dong. Region level based multi-focus image fusion using quaternion wavelet and normalized cut. *Signal Processing*, 97:9–30, 2014. DOI: 10.1016/j.sigpro.2013.10.010.

S. Mallat. *A Wavelet Tour of Signal Processing: The Sparse Way*, chapter 1 - Sparse Representations, pages 1–31. Elsevier B. V., 3rd edition, 2009. DOI: 10.1016/B978-0-12-374370-1.00005-7.

S. G. Mallat. A theory for multiresolution signal decomposition: the wavelet representation. *IEEE Transactions on Pattern Analysis and Machine Intelligence*, 11(7):674–693, 1989a. DOI: 10.1109/34.192463.

S. G. Mallat. Multiresolution approximations and wavelet orthonormal bases

of $L^2(\mathbb{R})$. *Transactions of the American Mathematical Society*, 315(1):69–87, 1989b. DOI: 10.2307/2001373.

Y. Meyer. *Wavelets and operators*, volume 37 of *Cambridge Studies in Advanced Mathematics*. Cambridge University Press, 1992 English edition. DOI: 10.1017/CBO9780511623820.

M. Mitrea. *Clifford Wavelets, Singular Integrals and Hardy Spaces*, volume 1575 of *Lecture Notes in Mathematics*. Springer Berlin Heidelberg, 1994. DOI: 10.1007/BFb0073556.

A. J. Morris. *Fourier and Wavelet Analysis of Clifford-Valued Functions*. Phd, University of Newcastle, Callaghan, New South Wales, Australia, 2014. Link: http://hdl.handle.net/1959.13/1041562.

C. Mosquera-Lopez, S. Agaian, and A. Velez-Hoyoz. The development of a multi-stage learning scheme using new tissue descriptors for automatic grading of prostatic carcinoma. In *Proceedings of the 2014 International Conference on Acoustics, Speech and Signal Processing (ICASSP 2014), held in Florence, Italy*, pages 3586–3590. IEEE, 2014. DOI: 10.1109/ICASSP.2014.6854269.

E. U. Moya-Sánchez and E. Bayro-Corrochano. Quaternion atomic function wavelet for applications in image processing. In *Progress in Pattern Recognition, Image Analysis, Computer Vision, and Applications: Proceedings of the 15th IberoAmerican Congress on Pattern Recognition (CIARP 2010), held in São Paulo, Brazil*, volume 6419 of *Lecture Notes in Computer Science*, pages 346–353. Springer Berlin Heidelberg, 2010. DOI: 10.1007/978-3-642-16687-7_47.

M. Naouai, A. Hamouda, A. Akkari, and C. Weber. New approach for road extraction from high resolution remotely sensed images using the quaternionic wavelet. In *Pattern Recognition and Image Analysis: Proceedings of the*

5th Iberian Conference on Pattern Recognition and Image Analysis (IbPRIA 2011) held in Las Palmas de Gran Canaria, Spain, volume 6669 of *Lecture Notes in Computer Science*, pages 452–459. Springer Berlin Heidelberg, 2011. DOI: 10.1007/978-3-642-21257-4_56.

S. Olhede and G. Metikas. The monogenic wavelet transform. *IEEE Transactions on Signal Processing*, 57(9):3426–3441, 2009. DOI: 10.1109/TSP.2009.2023397.

H. Pang, M. Zhu, and L. Guo. Multifocus color image fusion using quaternion wavelet transform. In *Proceedings of the 2012 5th International Congress on Image and Signal Processing (CISP 2012), held in Chongqing, China*, pages 543–546. IEEE, 2012. DOI: 10.1109/CISP.2012.6469884.

L. Peng and J. Zhao. Quaternion-valued smooth orthogonal wavelets with short support and symmetry. In *Advances in Analysis and Geometry*, Trends in Mathematics, pages 365–376. Birkhäuser Basel, 2004. DOI: 10.1007/978-3-0348-7838-8_18.

M. A. Pinsky. Brownian continuity modulus via series expansion. *Journal of Theoretical Probability*, 14(1):261–266, 2001. DOI: 10.1023/A:1007837502471.

R. A. Priyadharshini and S. Arivazhagan. A quaternionic wavelet transform-based approach for object recognition. *Defence Science Journal*, 64(4):350–357, 2014. DOI: 10.14429/dsj.64.4503.

N. Ricker. Wavelet contraction, wavelet expansion, and the control of seismic resolution. *Geophysics*, 18(4):769–792, 1953. DOI: 10.1190/1.1437927.

S. Sangeetha, C. M. Sujatha, and D. Manamalli. Anisotropic analysis of trabecular architecture in human femur bone radiographs using quater-

nion wavelet transforms. In *Proceedings of the 2014 36th Annual International Conference of the IEEE Engineering in Medicine and Biology Society (EMBC 2014), held in Chicago, IL*, pages 5603–5606. IEEE, 2014. DOI: 10.1109/EMBC.2014.6944897.

S. J. Sangwine. On harmonic analysis of vector-valued signals. *Mathematical Methods in the Applied Sciences*, 2016. DOI: 10.1002/mma.3938.

B. Sathyabama. *Development of novel texture analysis algorithms using photometric and geometric invariant features*. PhD, Anna University, Chennai, India, 2011. Link: http://hdl.handle.net/10603/25534.

B. Sathyabama, P. Chitra, V. G. Devi, S. Raju, and V. Abhaikumar. Quaternion wavelets based rotation, scale and translation invariant texture classification and retrieval. *Journal of Scientific and Industrial Research*, 70(4):256–263, 2011. NOPR: nopr.niscair.res.in/handle/123456789/11583.

I. W. Selesnick, R. G. Baraniuk, and N. G. Kingsbury. The dual-tree complex wavelet transform. *IEEE Signal Processing Magazine*, 22(6):123–151, 2005. DOI: 10.1109/MSP.2005.1550194.

Y. Shen, H. Feng, Q. Wang, Y. Liu, and Z. He. QWT enhanced SVM for hyperspectral image classification. In *Proceedings of the 2014 IEEE International Conference on Instrumentation and Measurement Technology (I2MTC 2014), held in Montevideo, Uruguay*, pages 1454–1458. IEEE, 2014. DOI: 10.1109/I2MTC.2014.6860986.

L. Shi. Exploration in quaternion colour. MSc dissertation, Simon Fraser University, Burnaby, Canada, 2005. Link: http://summit.sfu.ca/item/9829.

R. Soulard and P. Carré. Quaternionic wavelets for texture classification. In *Proceedings of the 2010 IEEE International Conference on Acoustics, Speech,*

and Signal Processing (ICASSP 2010), held in Dallas, USA, pages 4134–4137. IEEE, 2010a. DOI: 10.1109/ICASSP.2010.5495732.

R. Soulard and P. Carré. Quaternionic wavelets for image coding. In *Proceedings of the 18th European Signal Processing Conference (EUSIPCO 2010), held in Aalborg, Denmark*, pages 125–129. European Association for Signal, Speech, and Image Processing, 2010b. HAL: hal-00514423.

R. Soulard and P. Carré. Quaternionic wavelets for texture classification. *Pattern Recognition Letters*, 32(13):1669–1678, 2011. DOI: 10.1016/j.patrec.2011.06.028.

R. Soulard, P. Carré, and C. Fernandez-Maloigne. Vector extension of monogenic wavelets for geometric representation of color images. *IEEE Transactions on Image Processing*, 22(3):1070–1083, 2013. DOI: 10.1109/TIP.2012.2226902.

J.-O. Strömberg. A modified Franklin system and higher order spline systems on $\mathbb{R}^n$ as unconditional bases for Hardy spaces. In *Fundamental Papers in Wavelet Theory*, pages 197–215. Princeton University Press, 2006. Original paper from the Proceedings of the Conference on Harminic Analysis in Honor of Antoni Zygmund, held in Chicago, IL, in 1983 Link: http://www.jstor.org/stable/j.ctt7rt5v.34.

D. S. Taubman and M. W. Marcellin. JPEG2000: standard for interactive imaging. *Proceedings of the IEEE*, 90(8):1336–1357, 2002. DOI: 10.1109/JPROC.2002.800725.

A. Traoré, P. Carré, and C. Olivier. Reduced-reference metric based on the quaternionic wavelet coefficients modeling by information criteria. In *Proceedings of the 2014 IEEE International Conference on Image Processing (ICIP*

2014), held in Paris, pages 526–530. IEEE, 2014. DOI: 10.1109/ICIP.2014.7025105.

A. Traoré, P. Carré, and C. Olivier. Quaternionic wavelet coefficients modeling for a reduced-reference metric. *Signal Processing: Image Communication*, 36: 127–139, 2015. DOI: 10.1016/j.image.2015.06.003.

L. Traversoni. Quaternions on wavelets problems. In *Approximation Theory VIII*, volume 2: Wavelets and Multilevel Approximation of *Approximations and Decompositions vol. 6*, pages 391–397. World Scientific, Singapore, 1995. Not available online.

L. Traversoni. Quaternion wavelets for moving volume representation. In *Proceedings of the Fifth International Conference on Information Visualisation (IV 2001), held in London, UK*, pages 459–463. IEEE, 2001a. DOI: 10.1109/IV.2001.942096.

L. Traversoni. Image analysis using quaternion wavelets. In *Geometric Algebra with Applications in Science and Engineering*, chapter 16, pages 326–345. Birkhäuser, Boston, MA, 2001b. DOI: 10.1007/978-1-4612-0159-5_16.

L. Traversoni and Y. Xu. Velocity and object detection using quaternion wavelets. In *Proceedings of the 2007 International Conference on Numerical Analysis and Applied Mathematics (ICNAAM 2007), held in Corfu, Greece*, volume 936 of *AIP Conference Proceedings*, pages 775–778. American Institute of Physics, 2007. DOI: 10.1063/1.2790268.

M. Unser, D. Sage, and D. V. D. Ville. Multiresolution monogenic signal analysis using the RieszLaplace wavelet transform. *IEEE Transactions on Signal Processing*, 18(11):2402–2418, 2009. DOI: 10.1109/TIP.2009.2027628.

J. Ville. Théorie et applications de la notion de signal analytique. *Câbles et Transmission*, 2(1):61–74, 1948. Link: ark:/13960/t0wq37j28.

C. Wang, C. Zhao, and J. Yang. Monocular odometry in country roads based on phase-derived optical flow and 4-DOF ego-motion model. *Industrial Robot: An International Journal*, 38(5):509–520, 2011. DOI: 10.1108/01439911111154081.

C. Wang, C. Zhao, B. Fan, and J. Ding. Hyper-complex wave phase coherent based image motion estimation. In *Proceedings of the 32nd Chinese Control Conference (CCC 2013) held in Xi'an*, pages 3645–3650. IEEE, 2013. Link: http://ieeexplore.ieee.org/xpls/abs_all.jsp?arnumber=6640054&tag=1.

M. Weeks. *Digital Signal Processing using MATLAB and Wavelets*. Jones and Bartlett, Sudbury, MA, 2nd edition, 2011.

S. Wu, Q. Zhu, and Y. Xie. Evaluation of various speckle reduction filters on medical ultrasound images. In *Proceedings of the 35th Annual International Conference of the IEEE Engineering in Medicine and Biology Society (EMBC 2013), held in Osaka, Japan*, pages 1148–1151. IEEE, 2013. DOI: 10.1109/EMBC.2013.6609709.

X.-G. Xia and B. W. Suter. Vector-valued wavelets and vector filter banks. *IEEE Transactions on Signal Processing*, 44(3):508–518, 1996. DOI: 10.1109/78.489024.

Y. Xu, J. Zhou, and G. T. Zhai. 2-D phase-based matching in uncalibrated images. In *Proceedings of the 2005 IEEE Workshop on Signal Processing Systems (SiPS 2005), held in Athens, Greece*, pages 325–330. IEEE, 2005. DOI: 10.1109/SIPS.2005.1579887.

Y. Xu, X. Yang, P. Zhang, L. Song, and L. Traversoni. Cooperative stereo matching using quaternion wavelets and top–down segmentation. In *Proceedings of the 2007 IEEE International Conference on Multimedia and Expo (ICME 2007), held in Beijing, China*, pages 1954–1957. IEEE, 2007. DOI: 10.1109/ICME.2007.4285060.

Y. Xu, X. Yang, L. Song, L. Traversoni, and W. Lu. QWT: Retrospective and new applications. In *Geometric Algebra Computing in Engineering and Computer Science*, pages 249–273. Springer London, 2010. DOI: 10.1007/978-1-84996-108-0_13.

M. Yin, W. Liu, J. Shui, and J. Wu. Quaternion wavelet analysis and application in image denoising. *Mathematical Problems in Engineering*, 2012, 2012. Article no. 493976, DOI: 10.1155/2012/493976.

M. Yin, J. Wu, B. Chu, R. Kong, and Z. Wang. Multi-focus image fusion based on quaternion wavelet. *Journal of Information and Computational Science*, 11(9):3187–3198, 2014. DOI: 10.12733/jics20103882.

F. Yu, X. Liu, and L. Sun. Image denoising based on quaternion wavelet Q-HMT model. In *Proceedings of the 2014 33rd Chinese Control Conference (CCC 2014), held in Nanjing, China*, pages 6279–6282. IEEE, 2014. DOI: 10.1109/ChiCC.2014.6896020.

J. Zhao and L. Peng. Quaternion-valued admissible wavelets and orthogonal decomposition of $L^2(IG(2), \mathbb{H})$. *Frontiers of Mathematics in China*, 2(3): 491–499, 2007. DOI: 10.1007/s11464-007-0030-5.

J. M. Zhao and L. Z. Peng. Quaternion-valued admissible wavelets associated with the 2-dimensional Euclidean groupwith dilations. *Journal of Natural Geometry*, 20(1–2):21–32, 2001. Apparently not available online.

J. Zhou, Y. Xu, and X. Yang. Quaternion wavelet phase based stereo matching for uncalibrated images. *Pattern Recognition Letters*, 28(12):1509–1522, 2007. DOI: 10.1016/j.patrec.2007.03.009.

G. Zweig, R. Lipes, and J. R. Pierce. The cochlear compromise. *The Journal of the Acoustical Society of America*, 59(4):975–982, 1976. DOI: 10.1121/1.380956.